Universiteit
Leiden
The Netherlands

Superclusters

Oort, J.H.

Citation
Oort, J. H. (1983). Superclusters. *Annual Review Of Astronomy And Astrophysics*, *21*, 373-428.
Retrieved from https://hdl.handle.net/1887/7425

Version:	Not Applicable (or Unknown)
License:	Leiden University Non-exclusive license
Downloaded from:	https://hdl.handle.net/1887/7425

Note: To cite this publication please use the final published version (if applicable).

1983ARA&A..21..3730

Ann. Rev. Astron. Astrophys. 1983. 21: 373–428
Copyright © 1983 by Annual Reviews Inc. All rights reserved

SUPERCLUSTERS

J. H. Oort

Sterrewacht Leiden, Leiden, The Netherlands

1. INTRODUCTION

The distribution of galaxies is clumpy on all scales, ranging from binaries, triples, and multiples, through groups containing between a few and a hundred galaxies, to rich clusters with thousands of members, masses up to $10^{15\pm1}M_{\odot}$, and diameters of the order of 10 Mpc. The latter have been discussed by Neta A. Bahcall (5) in a preceding volume of this series. The clusters are at the end of the scale of the more or less regular structures in the Universe.

There exists also another type of galaxy agglomeration. These have diameters between roughly one and ten times those of large clusters, but have much smaller densities; they are usually irregular, with patchy density variations and no central concentration. The larger and most conspicuous of these agglomerations may contain several clusters, which explains why they have been given the name "superclusters." In their longer dimensions, crossing times exceed the age of the Universe. They are thus unrelaxed. Unrelaxed appearance, together with large size, might be taken as a definition of superclusters.

Inhomogeneity on the scale of the superclusters—up to ~ 100 Mpc[1]—shows up partly as density enhancements, but also as holes, in which the luminous density appears to be practically zero.

Although there can be no doubt about the reality of superclusters, their boundaries are often ill defined; it is sometimes hard to tell where one supercluster ends and another begins. It has even been hypothesized that they may all be interconnected, so that the Universe would consist of a

[1] For convenience a definite value of the Hubble constant, $H = 50\ \mathrm{km\ s^{-1}\ Mpc^{-1}}$, has been used throughout this article, rather than introducing the customary parameter h. The value of 50 was adopted on the strength of a recent discussion by Sandage & Tammann (72). It should be remembered that very different values, ranging up to $\sim 100\ \mathrm{km\ s^{-1}\ Mpc^{-1}}$, have been found in other investigations.

0066–4146/83/0915–0373$02.00

© Annual Reviews Inc. • Provided by the NASA Astrophysics Data System

1983ARA&A..21..3730

three-dimensional network of superclusters, with essentially empty meshes in between. Presently available data are, however, quite insufficient to trace such a network.

Nevertheless the study of superclusters is, in a sense, a study of the large-scale structure of the Universe.

In addition, such a study is important for three specific reasons:

1. Because of their largely unrelaxed state, superclusters may give an indication of the manner in which the largest structures in the Universe have originated; and, inasmuch as most galaxies may lie in superclusters, this might provide information on the epoch of galaxy formation.
2. Superclusters may contain information on the nature of the density fluctuations in the early Universe. The segregation of galaxy types in the Perseus supercluster (Section 5) seems to indicate that the galaxies were born during the formation of the supercluster itself, in the gaseous stage of the Universe. The absence of fluctuations in the microwave background radiation with amplitudes corresponding to supercluster masses presents a severe problem (Sections 9 and 10).
3. In the outskirts of a supercluster, the Hubble expansion is decelerated owing to the mass excess of the supercluster. Measurement of the average motion of galaxies in these outskirts relative to the gravitational center of the supercluster may provide an estimate of its mass and, indirectly, of the average density in the Universe. There are, however, many complications, which have so far impeded the derivation of a firm result.

Superclusters have been investigated by studying the distribution of galaxies and clusters on the sky, in combination with their radial velocities when available. In such studies a personal judgment is often inevitably involved. It is desirable to supplement it by a more objective approach. One such approach is to study the general correlation between positions of galaxies. This has been investigated extensively, especially by Peebles and collaborators (64, and references therein). The most generally used form is the so-called two-point correlation, or "co-variance" function $\xi(r)$ defined by

$$n(r) = \{1 + \xi(r)\}\,\langle n\rangle,$$

where $n(r)$ is the space number density of galaxies at a distance r from any given galaxy, and $\langle n\rangle$ is the general average density. Over a large range of r, ξ is found to follow a power law: $\xi = (r/r_0)^{-\gamma}$. The parameter r_0, the distance at which the density is twice the general average, has often been used as a measure for the clustering, and is called the clustering length. For small scales, $\gamma = 1.77$ and $r_0 \sim 10$ Mpc. It is remarkable that this simple

© Annual Reviews Inc. • Provided by the NASA Astrophysics Data System

1983ARA&A..21..3730

form of ξ describes the correlation over a range of r from 10 kpc to 10 Mpc, or perhaps even larger. The correlation function has proved to be extremely useful in providing such a unified description of the clumpiness. However, it is not suitable for describing the very long filamentary or flat structures that we encounter in superclusters, nor does it describe the large voids between these superclusters. Recently, attempts have been made by Zeldovich et al. (99) to obtain an impersonal quantitative description of superclustering, using notions from the "percolation theory" that are specially suited for establishing the presence of long chains (Section 9.1).

The present review, which is concentrated on the larger structures, begins with a description of some individual superstructures (Sections 3, 4.2, 5, 6, and 7). A general review of the characteristics of superclusters is given in Chapter 9; their frequency in space is considered in Section 4.3 and Chapter 7. In Chapter 10 scenarios for their possible origin are discussed.

2. HISTORICAL

Evidence of superclustering has existed since the earliest surveys of nebulae by the Herschels, which showed the striking excess of bright nebulae in the north galactic hemisphere due to the Virgo or Local supercluster, a feature later depicted so strongly in Shapley & Ames' (84) survey of bright galaxies (cf. Figure 1).

I do not intend to give a history of the subject, but a few early articles describing superclusters may be mentioned. In 1930, Shapley (81) gave an account of a "remote cloud of galaxies in Centaurus" at $13^{h}23^{m}.6 - 31^{\circ}.1$ (1900). He estimated it to be 14 times more distant than the "Coma-Virgo Cloud A." With the presently adopted distance for the Virgo cluster, his angular dimensions of $2^{\circ}.8 \times 0^{\circ}.8$ would then correspond to 14×4 Mpc. Another very large agglomeration, in Pisces, was described by Zwicky in 1937. It measured $13^{\circ} \times 4^{\circ}$ and encompassed several clusters.

Shapley's early papers were followed by numerous others dealing with the distribution of the galaxies found on (for that time) deep plates taken with the Bruce and Metcalf telescopes.

Evidence for the existence of large associations of galaxy clusters was first suggested by Abell on the basis of his systematic search for galaxy clusters on the plates of the National Geographic–Palomar Observatory Sky Survey (2). Abell listed a number of apparent associations, which he called class 2 clusters (3); their diameters averaged 70 Mpc (reduced to a Hubble constant of 50 km s^{-1} Mpc^{-1}) (cf. Section 7).

The first systematic surveys of faint galaxies were made by Hubble (46) and by Shane & Wirtanen (80). The former counted galaxies in a large number of small fields, while Shane & Wirtanen surveyed the whole sky

© Annual Reviews Inc. • Provided by the NASA Astrophysics Data System

1983ARA&A..21..3730

north of $-23°$ down to a limiting photographic magnitude of ~ 18.3. They found numerous dense clusters and groups, but also a general tendency of the nebulae to lie in structures with average dimensions of about 4°, corresponding to roughly 40 Mpc [Neyman et al. (56); cf. also Groth & Peebles (42), and references therein].

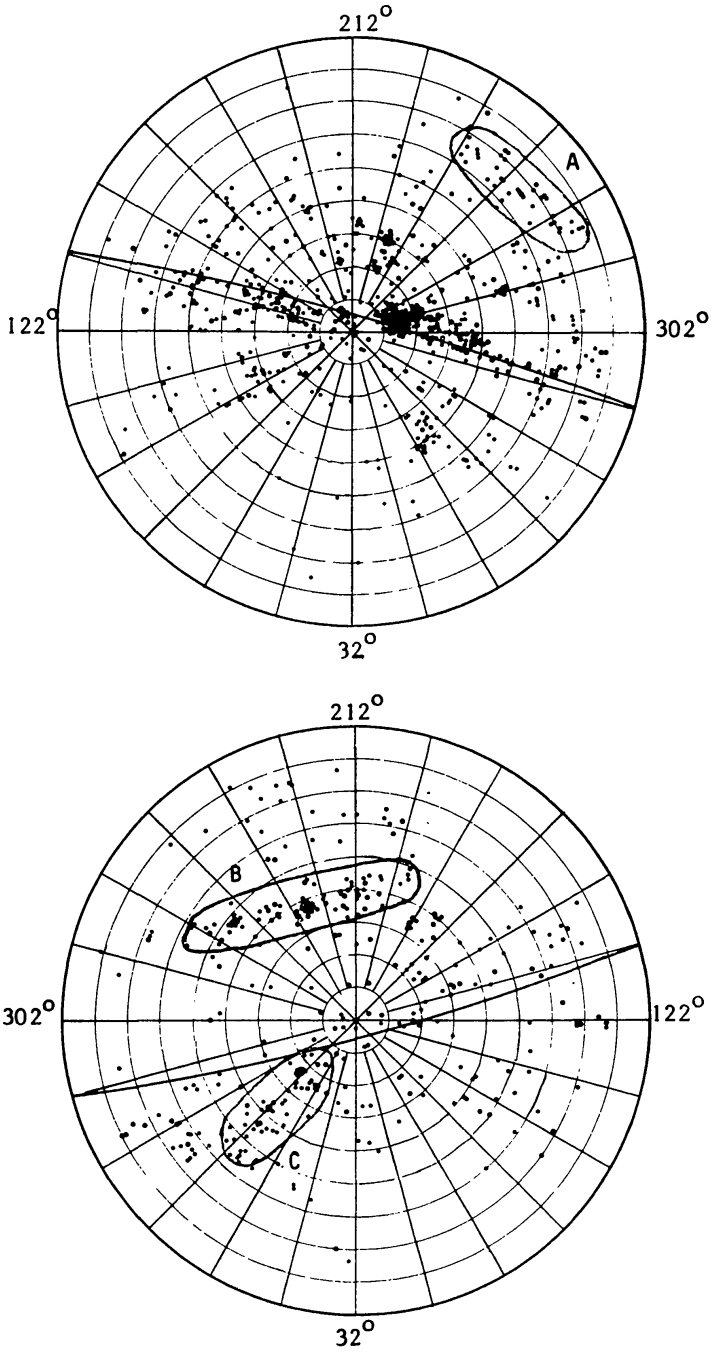

Figure 1 The distribution of galaxies brighter than the 13th photographic magnitude. The upper panel shows the north galactic hemisphere, the lower the south galactic hemisphere. The galactic poles are at the centers, the circles are at intervals of 10° latitude; ℓ^{II} is shown at the circumference [adapted from Shapley & Ames (84)].

© Annual Reviews Inc. • Provided by the NASA Astrophysics Data System

1983ARA&A..21..3730

Shane (79) gave a detailed description of some special concentrations or "clouds" that stand out in the large survey. Figure 2 shows an example. It contains 12 galaxy clusters listed by Abell and at least 1 other cluster that appear to lie in the same distance range. The average velocity is 22,000 km s^{-1}, corresponding to a distance of 440 Mpc (for $H = 50$).

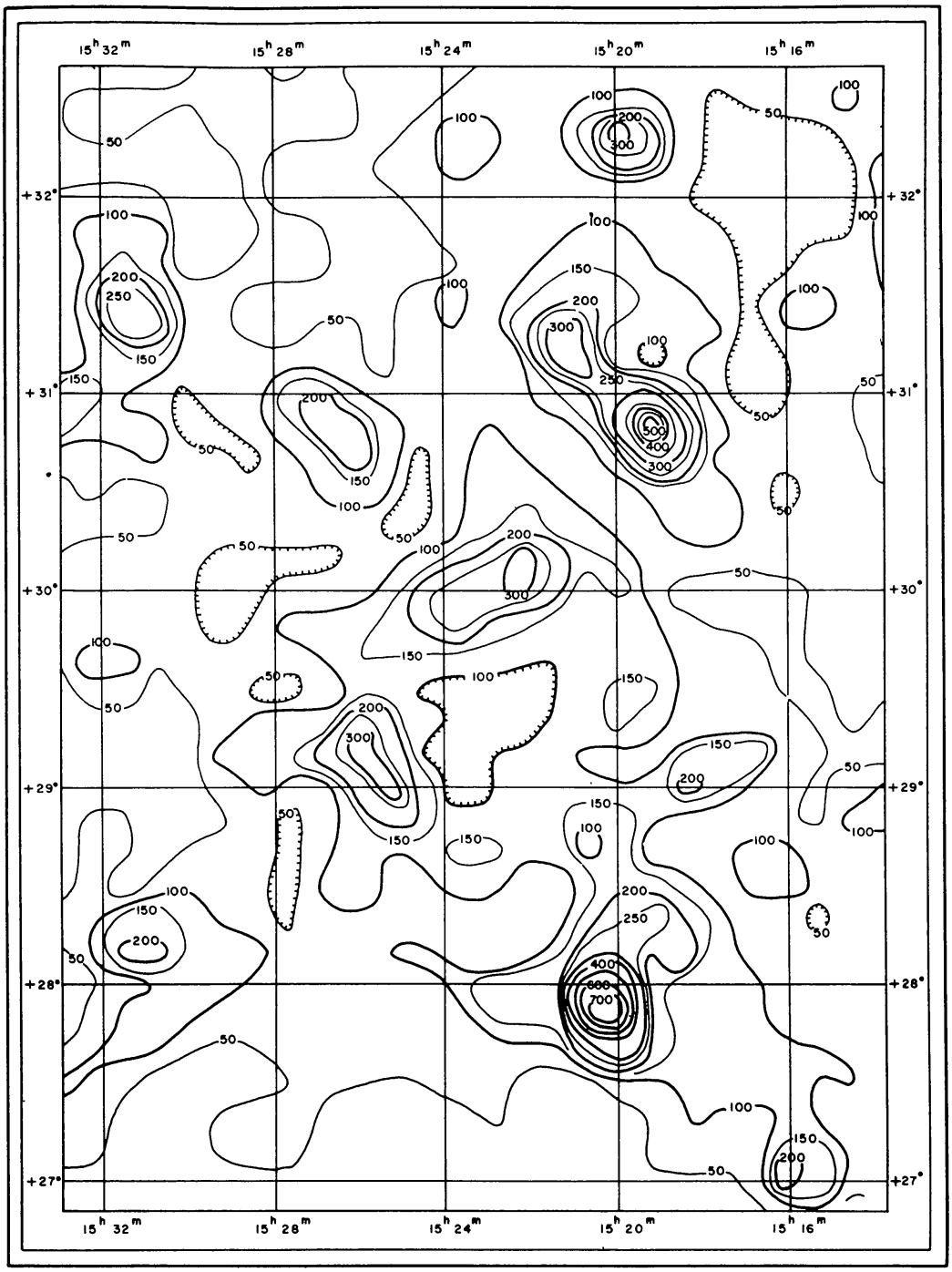

Figure 2 A concentration of galaxies and clusters in Corona, from the survey by Shane & Wirtanen. Contour values represent number of galaxies per square degree. [Shane (79.]

© Annual Reviews Inc. • Provided by the NASA Astrophysics Data System

1983ARA&A..21..3730

A new era for the study of superclusters started with the advent of greatly improved spectrographs and emulsions for measuring radial velocities of relatively faint galaxies. Some of the first results are discussed in the sections that follow.

3. DISTRIBUTION AND MOTIONS OF THE GALAXIES DOWN TO THE 13TH PHOTOGRAPHIC MAGNITUDE; THE VIRGO, OR LOCAL, SUPERCLUSTER

A good impression of the characteristics of a supercluster may be obtained by studying the structure and motions of our own supercluster.

Figure 1 shows the distribution of approximately 1280 galaxies brighter than about the 13th photographic magnitude taken from a 1938 paper by Harlow Shapley and Adelaide Ames. Striking features are the Virgo cluster at $\ell = 280°.4$, $b = +74°.6$ (galactic coordinates on the new system), with a distance ~ 20 Mpc, a diameter ~ 2.0 Mpc, a tail around $\ell = 305°$ stretching from $b \sim +70°$ to $b \sim +50°$, and an opposite elongated appendage extending from a region close to the galactic pole to $\ell \sim 140°$, $b \sim +50°$ (the so-called Ursa Major cluster). Merely on the basis of the distribution on the sky, there can be little doubt that these features are associated. The connection is fully corroborated by the extensive photometric and radial-velocity data that have recently become available [Sandage & Tammann (71), Tully (92)]. The velocity of the Ursa Major tail is slightly smaller than that of the opposite tail. Both have a relatively small spread in velocity.

The distribution of the bright galaxies over the whole sky is extremely clumpy, with groups varying between a few and ten or twenty members, and of various dimensions. De Vaucouleurs (20) has given a comprehensive list and description of 54 groups. These groups are sometimes arranged in ridges somewhat like the 80°-long ridge through the Virgo cluster and its appendages. De Vaucouleurs (21) has discussed the possibility of rotation of the Local supercluster. The issue is not clear, complicated among other things by the obvious deviations from symmetry and the difficulty of distinguishing between effects of distance and systematic motion.

The north galactic hemisphere is clearly more densely populated than the southern, even if we leave out the Virgo cluster and its appendages. The majority of all the galaxies in this hemisphere may belong to one superstructure. This is distinctly flattened toward an axis identical with that of the dense chain containing the Virgo cluster. This axis has been termed the supergalactic equator by de Vaucouleurs, and is shown by a curve in Figure 1. The galaxies in the region between $\ell \sim 240°$ and 280°, b between $+12°$ and $+30°$ (marked by contour A) may form a separate system; its

© Annual Reviews Inc. • Provided by the NASA Astrophysics Data System

1983ARA&A..21..3730

velocity relative to the Local Group is ~ 2500 km s^{-1}, as against 1070 km s^{-1} for the Virgo cluster.

It is not clear how far the Virgo supercluster extends beyond the Sun. As shown in Figure 1, the two most striking features in the south galactic hemisphere do not fit at all to the supergalactic equator. The most obvious deviating "filament" is that around $b = -50°$ between 200° and 270° longitude, noted by de Vaucouleurs (19) and indicated by a contour line marked B in Figure 1. I shall refer to it as the "south galactic chain." It has a velocity of 1400 km s^{-1}, a velocity dispersion of ~ 300 km s^{-1}, and might be considered as a separate supercluster, with a length of ~ 30 Mpc and an axial ratio of $\sim 6:1$ in projection. A further feature deviating strikingly from the supergalactic equator stretches from the south galactic pole along $\ell \sim 350°$ (contour C). The part between $b = -20°$ and $-50°$ has an average velocity of ~ 3500 km s^{-1}, and probably lies well outside the Local supercluster.

All three features have major diameters of ~ 30 Mpc, and may well be considered as separate superclusters. This would give a number density of 2–3 superclusters per 10^6 Mpc^3, comparable to the densities estimated in Section 4.

The whole structure in the south galactic hemisphere is so erratic that the nature of the connection with the central Virgo complex remains uncertain. However, if we leave out the south galactic chain the galaxies in this hemisphere do show a tendency for concentration to the supergalactic equator: there are 182 with $B > 30°$ as against 603 with $B < 30°$. This seems to show that the supercluster does extend considerably beyond the Galaxy. (B is de Vaucouleurs' supergalactic latitude; his supergalactic longitude L is counted along the supergalactic equator from its intersection with the galactic equator at $\ell = 137°$.) The Virgo cluster has $L = 102°$, $B = -3°$. See the legends to Figures 3 and 4 for a definition of the directions of supergalactic coordinates.

The most pronounced feature of our supercluster remains the Virgo cluster itself with its two opposite extensions. At the outer end of the "southern extension" (toward higher L) is a cluster with a velocity around 2500 km s^{-1}; as its distance appears to be about twice that of the Virgo cluster proper, it probably does not belong to the inner structure of the supercluster. The longer tail extending to smaller L, containing the so-called Ursa Major cluster, has only a few velocities higher than 2000 km s^{-1}, and appears to lie at the same distance as the cluster. The entire "central" structure is approximately 70° (or ~ 28 Mpc) long and has an apparent axial ratio of about 1:10; it may either be an oblate distribution seen roughly edge-on, or possibly a prolate feature.

Another notable characteristic is the presence of large, empty regions in both hemispheres. In the zone below 20° latitude the absence of galaxies is

© Annual Reviews Inc. • Provided by the NASA Astrophysics Data System

1983ARA&A..21..3730

due to galactic absorption, but there are clearly several other empty regions in Figure 1, indicating that large volumes of space are practically devoid of luminous matter.

There is a striking difference in composition between the central cluster and all other features; the dense concentration in the cluster consists exclusively of E and S0 galaxies, while the "tails" have about 25% of E and S0, and the rest of the supercluster about 44%.

The first extensive discussion of the Local supercluster was given by de Vaucouleurs (19). It was followed by a number of other articles by him and collaborators. References may be found in the review given in the IAU Symposium No. 79 [de Vaucouleurs (21)].

Much work has been done on the radial velocities. In the cluster itself they show a relatively high dispersion, $\sigma = 650$ km s^{-1}, and the motions appear to be largely randomized; the crossing time is roughly 2×10^9 yr. The large supercluster, however, must be essentially unmixed, the crossing time being of the order of 5 Hubble times for parts 20 Mpc from the center.

New descriptions of the Local supercluster, based on space coordinates derived from radial velocities, have been given by Yahil et al. (96) and by Tully (92). Velocities were taken from the *Revised Shapley-Ames Catalog* [RSA: Sandage & Tammann (71)] or, in Tully's case, from data in the *Atlas and Catalog of Nearby Galaxies* [NBG: Fisher & Tully (32)]. Yahil et al. published stereoscopic views displaying the structure of the supercluster, and derived values for its gravitational field at the position of the Sun. Tully made a detailed study of the space distribution assuming that outside the Virgo cluster itself deviations from the Hubble flow are relatively small, so that individual distances can be computed from radial velocities. The investigation was preliminary; for instance, no account was taken of the deviations from the Hubble flow caused by the attraction of the supercluster. Most of the features discussed in the following are little affected by the distance errors due to this neglect. The most serious effects occur in Figure 4, where they have contributed to the apparent hole behind the Virgo cluster.

Plots in rectangular coordinates are shown in Figures 3, 4, and 5 [from Tully (92)]. The coordinate system corresponds to de Vaucouleurs' supergalactic latitude and longitude. The Sun is at the center. The Virgo cluster lies roughly in the direction of the *SGY*-axis; the *SGZ*-axis is perpendicular to the supergalactic plane. Figure 5 contains only the galaxies in the north galactic hemisphere ($b^{II} > 0°$). It shows, on one hand, the concentration of these galaxies in a thin layer coinciding with the supergalactic plane and, on the other hand, a wide distribution in what Tully refers to as the halo. The striking concentration in the plane and the rather clear distinction between the three components "Virgo cluster,"

© Annual Reviews Inc. • Provided by the NASA Astrophysics Data System

1983ARA&A..21..3730

"disk," and "halo" is further illustrated in Figure 6, likewise from Tully, showing the distribution of all NBG galaxies brighter than $M_B = -19.5$ in a cylinder perpendicular to the supergalactic plane with a radius of about 20 Mpc around the Virgo cluster. The cluster itself has been omitted.

Tully estimates that of the NBG material roughly 60 % belong to the cluster and the disk, and 40% to the halo.

Besides the Virgo cluster, the disk contains the two extended clouds that have been referred to previously: one extending toward the right in Figure 5, which contains the Ursa Major cluster (referred to as Canes Venatici cloud in Tully's article), the other toward the left (referred to as the southern extension, or, alternatively, as the Virgo II cloud). Taken together, these clouds show a structure flattened in the ratio $SGX:SGY:SGZ = 6:3:1$. Distance errors have negligible effects on the SGZ-coordinate and relatively small effects on the SGX-coordinate, so that the ratio of the long and short axes deserves some confidence. It is at least 6:1. The overall shape of the disk component is more oblate than prolate. The dispersion in the SGZ direction is $\sigma_Z = 2.2$ Mpc, if $H = 50$.

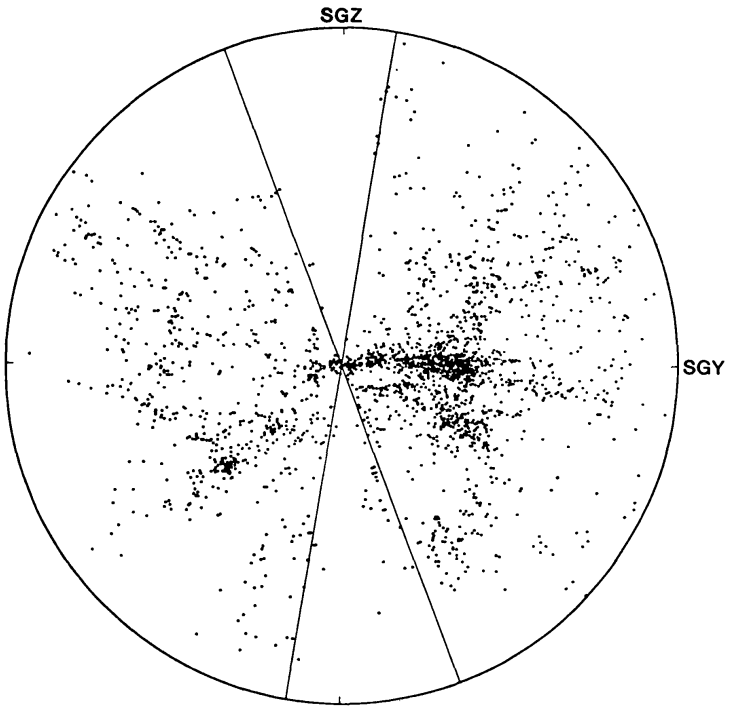

Figure 3 All 2175 galaxies in the Nearby Galaxy Catalog (NBG) projected onto the SGY-SGZ plane. The SGY-axis is directed toward supergalactic longitude 90°, supergalactic latitude 0° ($\ell^{II} = 227°$, $b^{II} = +83.^\circ7$), the SGZ-axis toward supergalactic latitude 90° ($\ell^{II} = 47.^\circ4$, $b^{II} = +6.^\circ3$). The radius of the outer boundary is 60 Mpc. The galactic zone of avoidance ($b < 15°$) is contained within the opposed wedges tilted by 6° with respect to the SGZ-axis. There is a zone of incompletion ($\delta < -45°$), which is projected across most of the southern supergalactic hemisphere. Figures 3–6 are reproduced by courtesy of R. B. Tully (92).

© Annual Reviews Inc. • Provided by the NASA Astrophysics Data System

1983ARA&A..21..3730

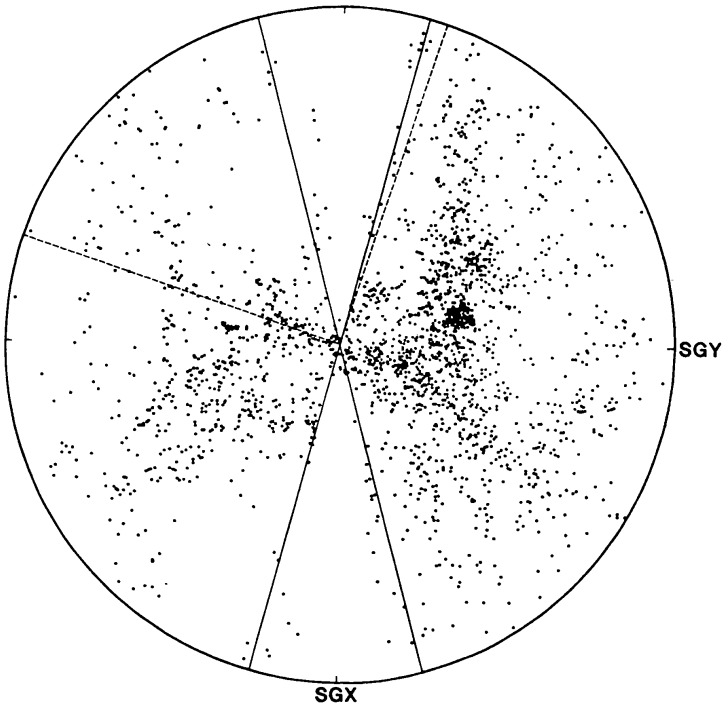

Figure 4 All galaxies in the NBG catalog projected onto the *SGX-SGY* plane. The *SGX*-axis is aligned toward supergalactic longitude 0°, latitude 0°. ($\ell^{II} = 137.^{\circ}2, b^{II} = -0.^{\circ}7$). The galactic zone of avoidance is symmetric about the *SGX*-axis. The large wedge occupying the upper-left quadrant locates the zone of incompletion.

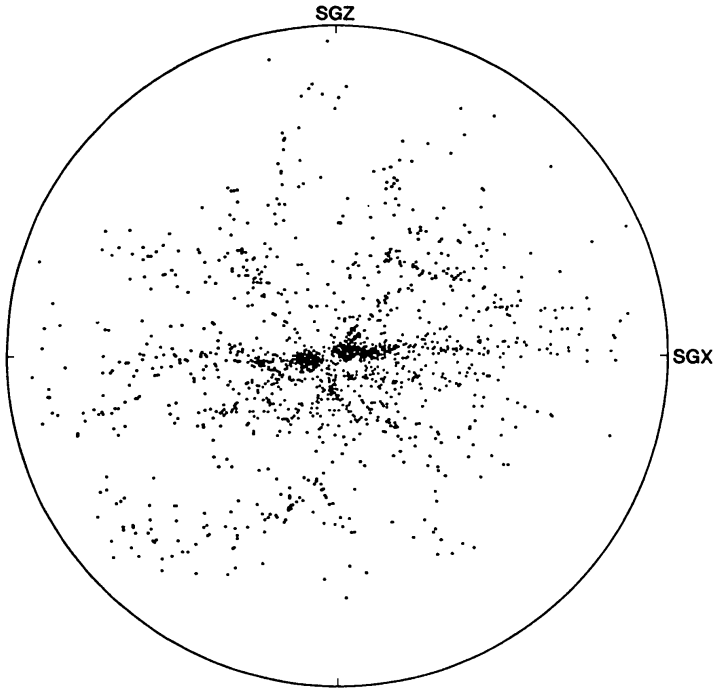

Figure 5 Projection on the *SGZ-SGX* plane for the galaxies in the north galactic hemisphere.

© Annual Reviews Inc. • Provided by the NASA Astrophysics Data System

1983ARA&A..21..3730

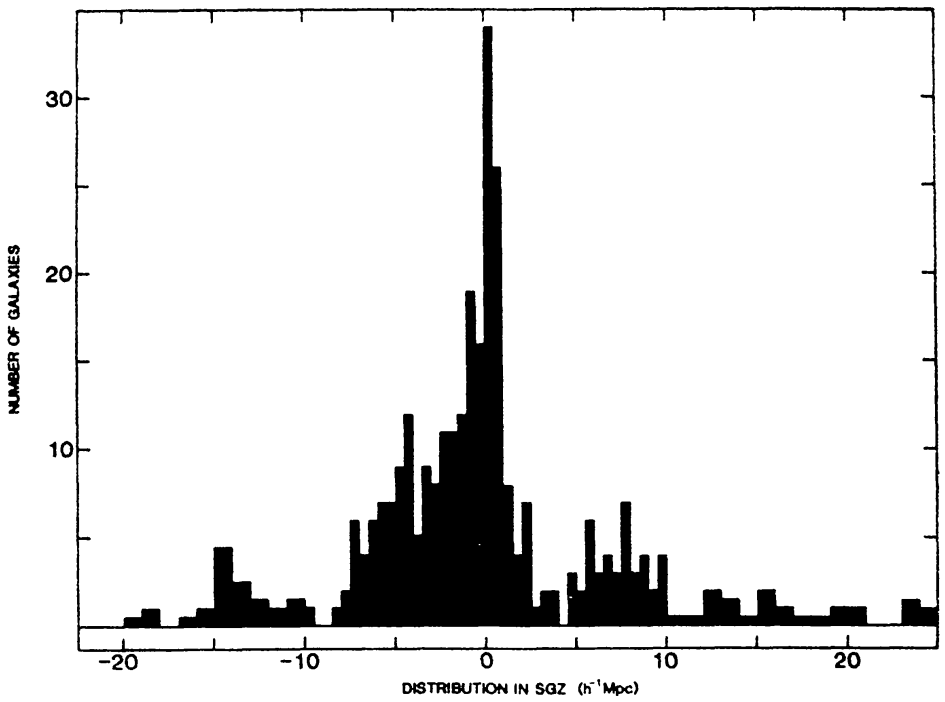

Figure 6 The distribution of Tully & Fisher's NBG galaxies in the surroundings of the Virgo cluster normal to the plane of the Local supercluster. Included are all galaxies with SGX between -20 and $+20$ Mpc, SGY between 0 and $+30$ Mpc, and corrected blue absolute magnitudes brighter than -19.5. The galaxies associated with the 12° diameter Virgo cluster (at $SGX = -4$, $SGY = +20$) have been excluded [after Tully (92), with his kind permission].

The general distribution in the disk can best be judged from Figure 4. It shows great deviations from circular symmetry around the Virgo center, which can only partly be attributed to galactic absorption or to systematic distance errors.

Tully has drawn attention to a remarkable structure of the halo surrounding the Virgo cluster (cf. 92, Figures 8 and 10). His plots give the distribution of galaxies in a slab through the Virgo cluster perpendicular to the SGY-axis and extending in SGY from roughly $+18$ to $+34$ Mpc. The distribution in this halo appears extremely uneven. The great majority of the galaxies lie in a small number of "clouds." Most of the space is empty. The three principal halo clouds as well as the minor concentration in the first quadrant have strikingly elongated shapes, which seem to point toward the Virgo cluster. Tully suggests that these shapes are due to the gravitational action of the cluster.

The volume density in the supercluster, averaged over all solid angles, falls off as R_V^{-2}, where R_V is the distance from the Virgo cluster (71, 96).

Internal motions in the various large clouds of which the Local supercluster consists seem generally to be so small (<100 km s^{-1}) that crossing times are longer than the age of the Universe. A similar result is

© Annual Reviews Inc. • Provided by the NASA Astrophysics Data System

1983ARA&A..21..3730

found when we consider the random motions of the groups relative to each other: not much mixing can have occurred in the supercluster as a whole.

There are indications of filamentary connections between the Virgo cluster and the Coma/Abell 1367 clusters [cf. Figure 7 from an article by Zeldovich et al. (99)]. The article also discusses a plot of the distribution in supergalactic Z of all galaxies within a cube of about 200 Mpc size contained in a catalog of galaxies with known velocities. This plot seems to indicate that the Local supercluster is part of a fluctuation on a still larger scale, the central plane of which coincides approximately with the supergalactic equator.

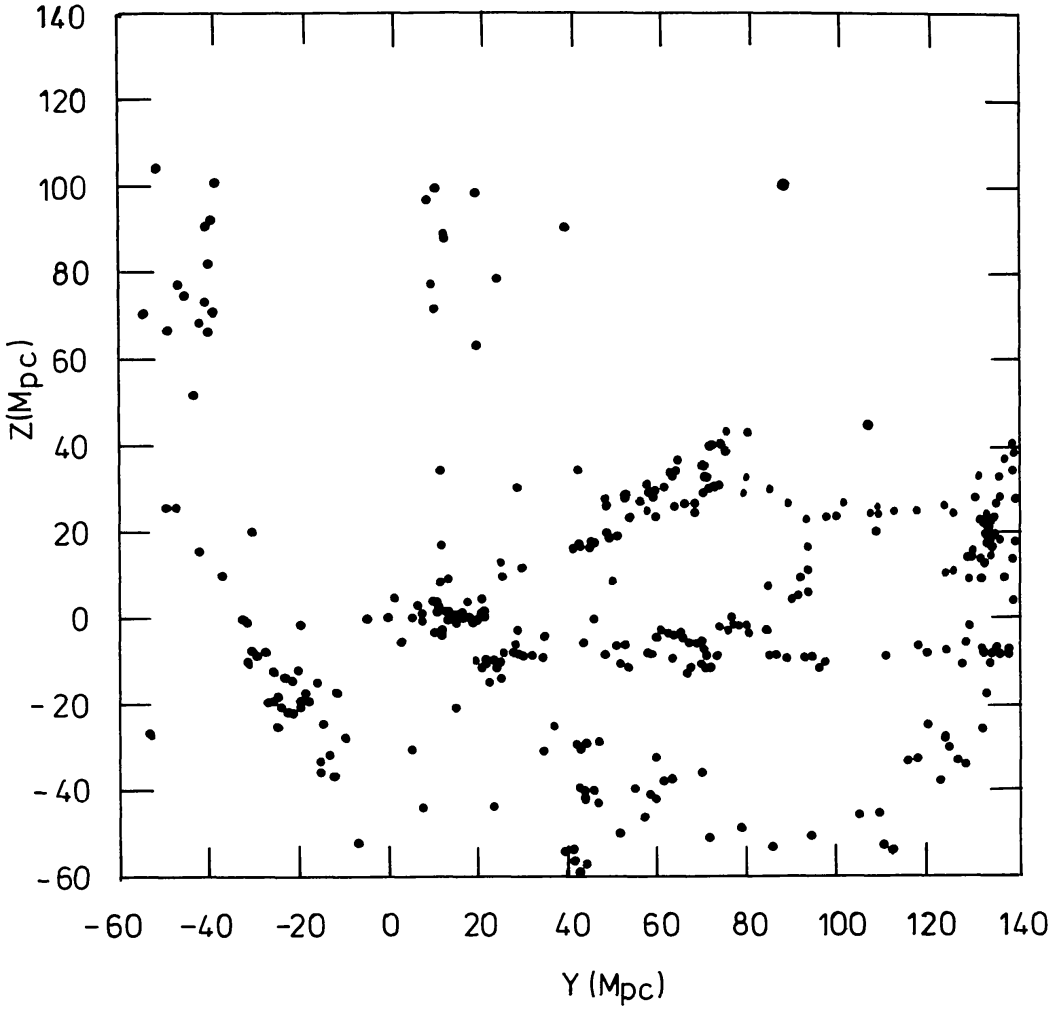

Figure 7 An indication of "strings" between the Virgo and Coma superclusters. The picture shows the distribution in supergalactic Y and Z of galaxies from a catalog of galaxies compiled by Huchra [as quoted by Zeldovich et al. (99)] in a slice between supergalactic $X = 0$ and $+10$. The Galaxy is at $X = Y = Z = 0$, the Virgo cluster lies at $Y = +20$, the Coma cluster is near the right-hand side at $Z = +20$, and A 1367 is at $Z = -10$. The figure is from an article by Zeldovich et al. (99).

© Annual Reviews Inc. • Provided by the NASA Astrophysics Data System

1983ARA&A..21..3730

4. THE NORTH GALACTIC POLAR CAP TO A DISTANCE OF 200 MPC

4.1 *Introduction*

The discussion in the preceding section was generally confined to a region within about 50 Mpc. For larger distances no data are available that cover the whole sky, but a great stride forward has been made by M. Davis et al. at the Harvard-Smithsonian Center for Astrophysics (16). They completed a redshift survey of all galaxies down to $m_B = 14.5$ in the north and south galactic polar caps above declination 0°, covering 2.7 ster [Huchra et al. (47)]. The magnitudes used are those given by Zwicky et al. (101). The authors gave plots in galactic coordinates for various velocity intervals. The plots for galaxies with galactocentric velocities between 3000 and 10,000 km s^{-1} and latitudes above +40° are shown in Figures 8 and 9, with separate symbols for five velocity intervals. More precise data on the velocities are shown in the right-ascension/velocity plots for five declination zones in Figures 10*a–e*. They amply illustrate the extreme clumpiness of the galaxy distribution in space and velocity. Davis et al. describe the situation as follows:

> The intermediate and distant redshift windows [i.e. those shown in Figures 8 and 9] exhibit clustering in frothy, almost filamentary, patterns of connectedness surrounding empty holes on the sky.... The transverse maps [these are maps like Figure 10] confirm the general impression that the large-scale clustering is characterized by connected features surrounding large holes often 20 Mpc [for $H = 100$ km s^{-1} Mpc^{-1}] or more across, both in the north and the south.

In their abstract, Davis et al. refer to large filamentary superclusters of up to 60 Mpc in extent (again for $H = 100$). In all these figures, only the galaxies brighter than −20.0 absolute magnitude (Zwicky scale of photographic magnitude; $H = 50$ km s^{-1} Mpc^{-1}) have been included. This makes them complete to the distance corresponding to 4000 km s^{-1}. For larger distances, they become increasingly incomplete. The real density in the more distant superclusters is therefore considerably larger than that indicated by the pictures.

4.2 *The Coma Supercluster*

Among the large conglomerations, the most striking is that indicated by the contour COMA in Figures 9, 10*b*, and 10*c*. It contains two rich clusters, Coma (Abell 1656, at $\alpha\ 12^h57^m$, $\delta + 28°.2$) and Abell 1367 ($\alpha\ 11^h42^m$, $\delta + 20°.6$), and will be referred to as the Coma supercluster. The densest part extends from $11^h.0$ +20°, 6200 km s^{-1}, to $13^h.6$ +35°, 7400 km s^{-1}, over a length of 37° on the sky, or 91 Mpc in space. With diminished density it may be

© Annual Reviews Inc. • Provided by the NASA Astrophysics Data System

1983ARA&A..21..3730

traced to $10^h + 18°$, 6000 km s^{-1} on the side of lower α, and to $15^h + 36°$, 9000 km s^{-1} in the direction of higher α. A recent plot of UCG galaxies [Nilson (57)] with velocities between 5000 and 8000 km s^{-1} indicates a filamentary extension up to $14^h7 + 33°$ (G. Vettolani, private communication)]. The total length would then be roughly 160 Mpc. The width on the sky is about 10°, which at the average distance of 136 Mpc of the supercluster corresponds to 24 Mpc. The axial ratio for the densest part is thus 0.27. If the extensions are included, the ratio is brought down to 0.15.

We have no information on the dimension along the line of sight. Figures 10*b*, 10*c*, and 12 show that outside the clusters the total width in velocity averages about 1000 km s^{-1}. But we cannot use this to determine the depth, because we do not know the rate of expansion within the supercluster, which depends on its unknown history (cf. Section 10).

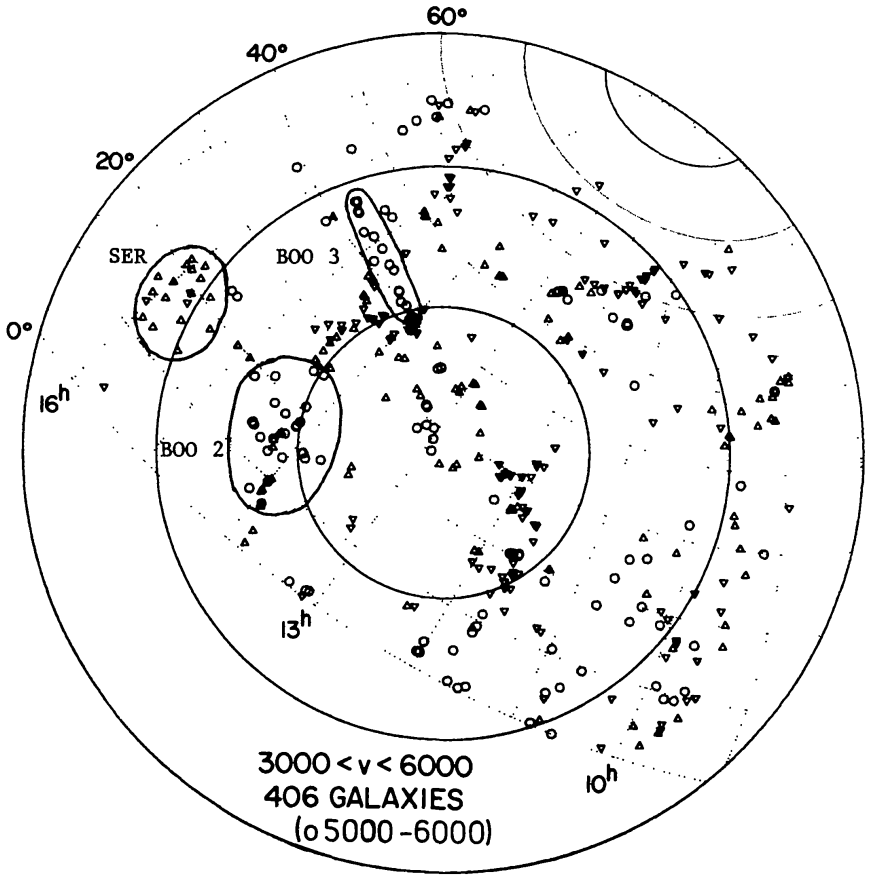

Figure 8 An equal-area plot in galactic coordinates of galaxies brighter than $m_B = 14.5$ above $b = +40°$. The galactic pole is at the center, the circles are at $b = 30°$, 50°, and 70°. Right ascensions and declinations are indicated by dotted curves. Galaxies whose absolute magnitudes are fainter than -20.0 (on the $H_0 = 50$ distance scale) have been omitted. The various symbols denote the following velocity bins: ▽ (3000–4000), △ (4000–5000), ○ (5000–6000 km s^{-1}). Reproduced by courtesy of M. Davis (except for the contours).

© Annual Reviews Inc. • Provided by the NASA Astrophysics Data System

1983ARA&A..21..3730

The supercluster may be oblate, with an axial ratio of the order of 1/5, but it may also be prolate. It is certainly far from spherical.

That the actual structure is more complicated than what is apparent in Figure 9 is illustrated by Figure 11 from an investigation by Fontanelli (34). It shows the surface distribution of galaxies inferred from the catalogs by Zwicky et al. (101) and by Nilson (57). The densest spot, at $12^h57^m + 28°.2$, is the Coma cluster. A ridge extends from this cluster to the upper right. From a determination of velocities in the roughly 3°-wide ridge and its surroundings, Fontanelli has shown that it is a distinct feature at a velocity of 7000 km s^{-1}, which coincides with that of the Coma supercluster. The filament makes a large angle with the main part of the supercluster, which extends from Coma toward Abell 1367 at $11^h42^m + 20°.6$.

The dense Coma cluster is strongly elongated. A recent investigation by Schipper & King (77) gives 65° for the position angle of its major axis. This coincides accurately with the direction from Coma to Abell 1367. It also coincides, as Fontanelli has remarked, with the direction from Coma to the

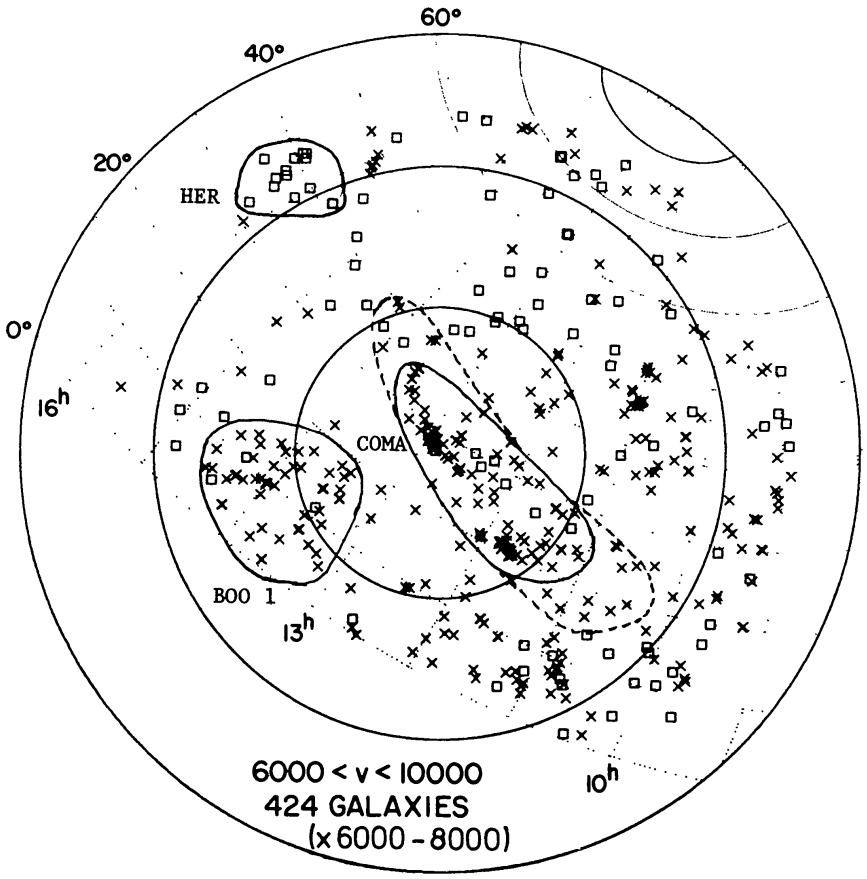

Figure 9 Same as for Figure 8, but for velocities between 6000 and 10,000 km s^{-1}. Symbols: × (6000–8000), □ (8000–10,000 km s^{-1}).

© Annual Reviews Inc. • Provided by the NASA Astrophysics Data System

1983ARA&A..21..3730

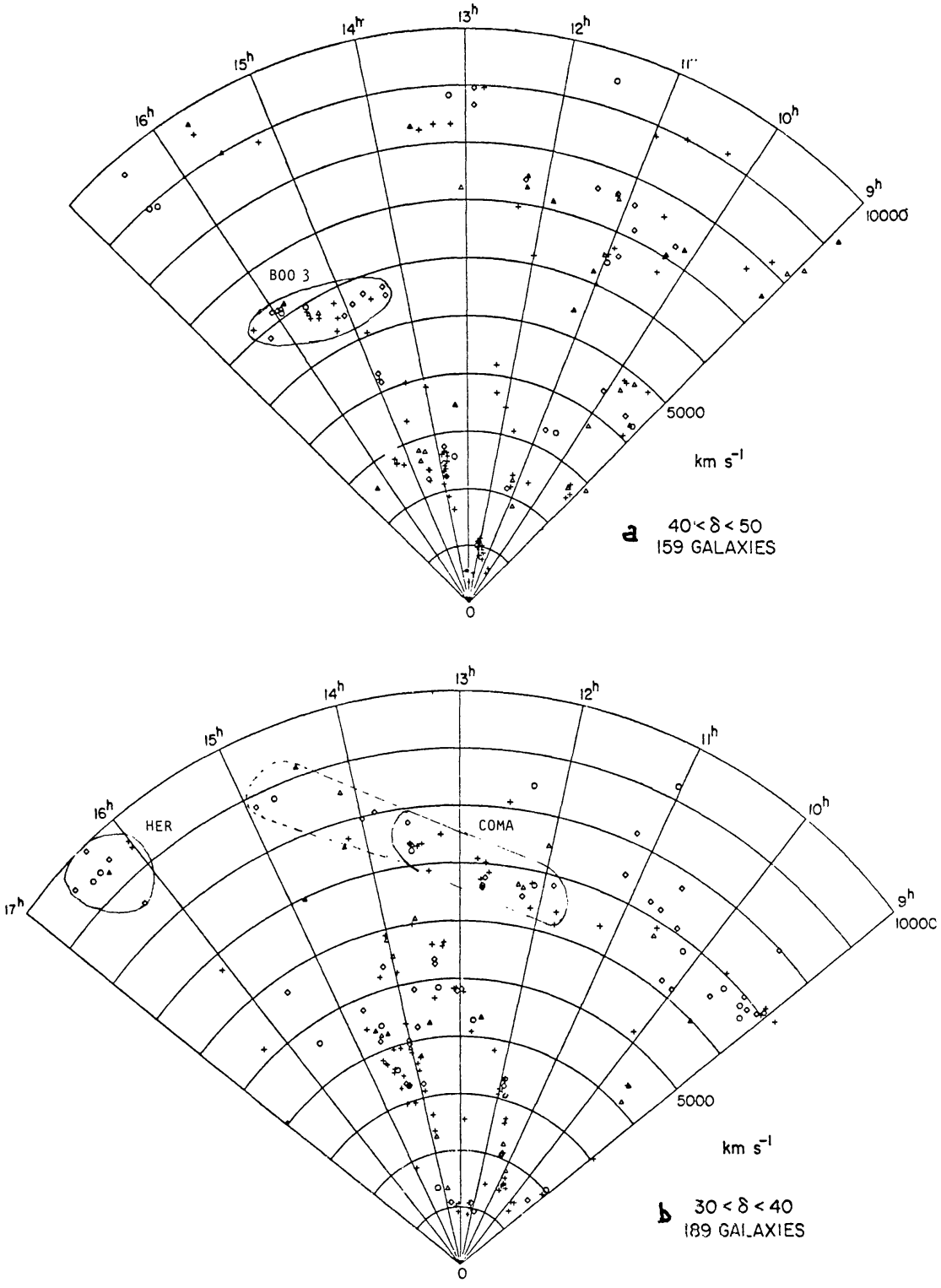

Figure 10 Distribution of galaxies with $m_B < 14.5$ in right ascension and velocity for five declination zones. Different symbols denote galaxy types: ○ (ellipticals), ◇ (S0), + (spirals), △ (irregulars). Again, galaxies fainter than $M_B = -20.0$ were omitted. Courtesy of M. Davis; contours were drawn in by the present author.

© Annual Reviews Inc. • Provided by the NASA Astrophysics Data System

1983ARA&A..21..3730

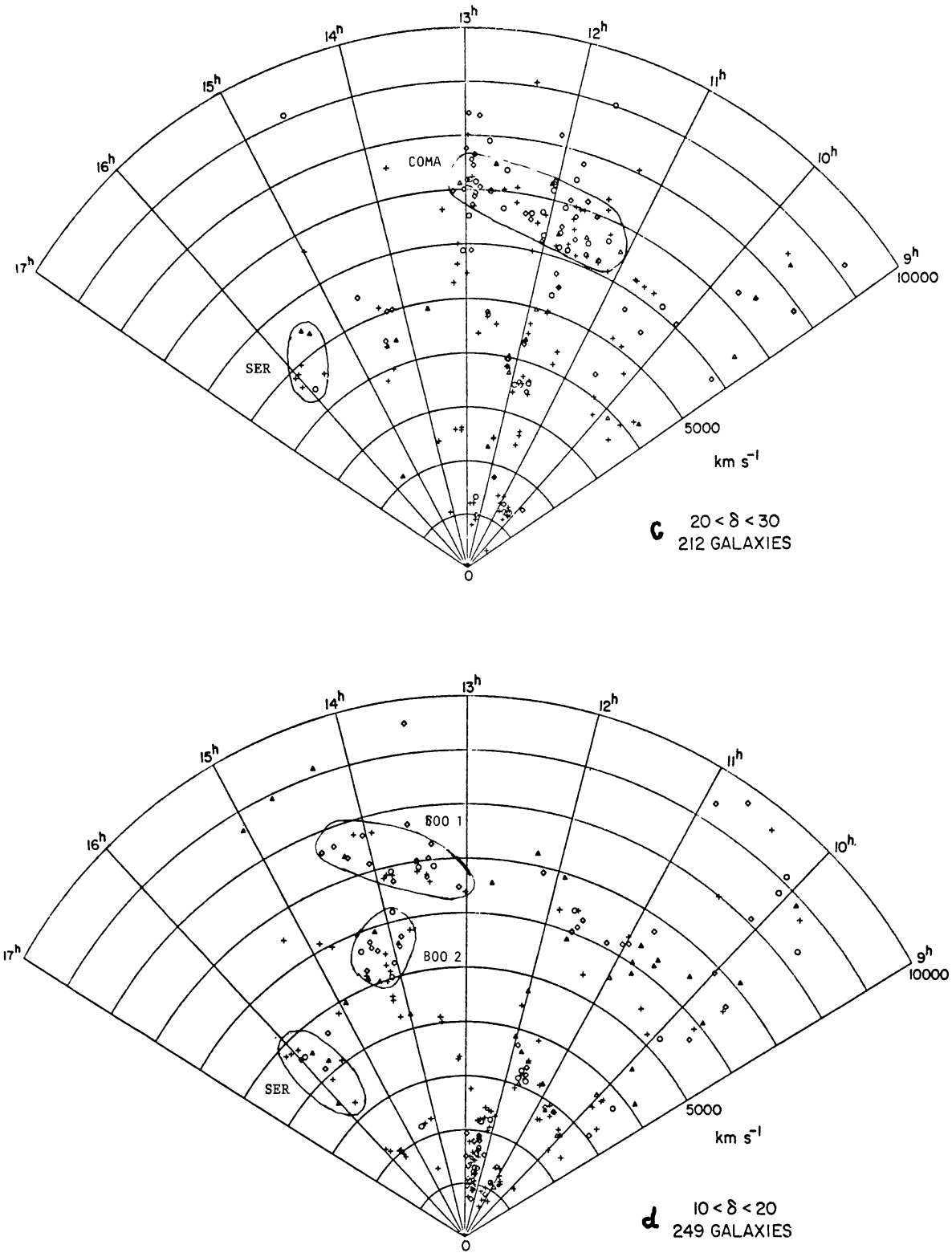

Figure 10 (*continued*)

© Annual Reviews Inc. • Provided by the NASA Astrophysics Data System

1983ARA&A..21..3730

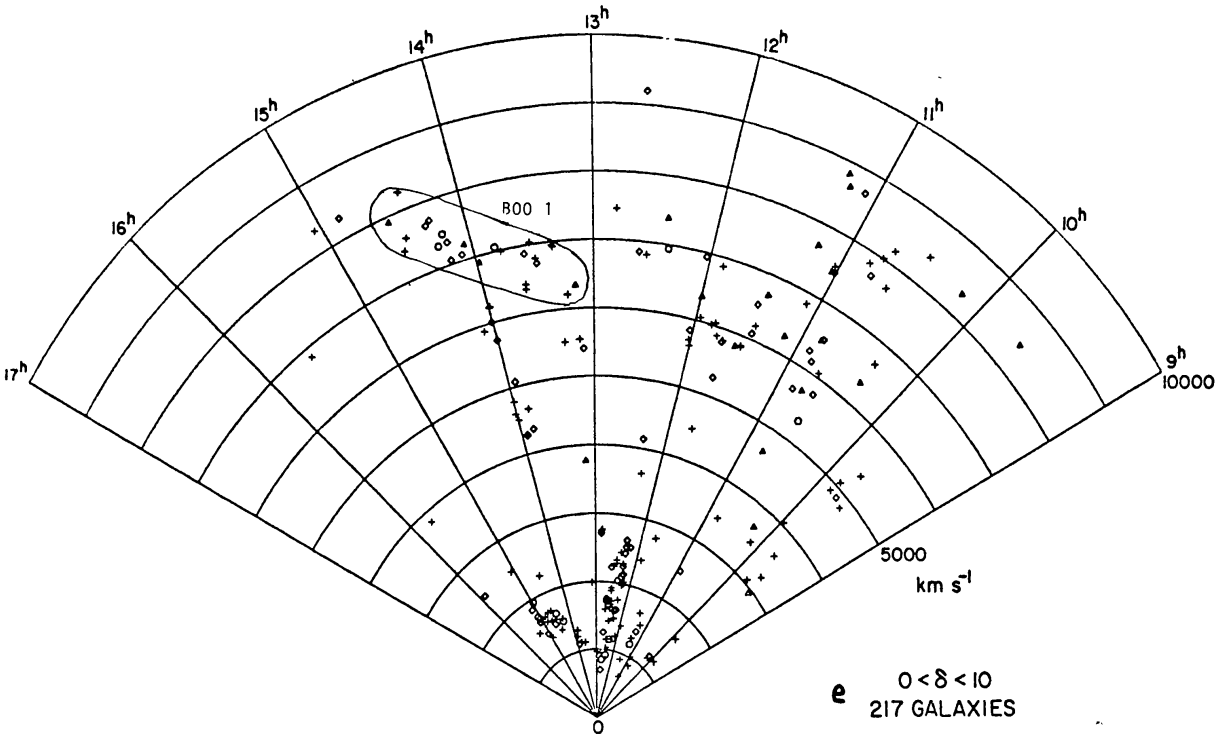

Figure 10 (continued)

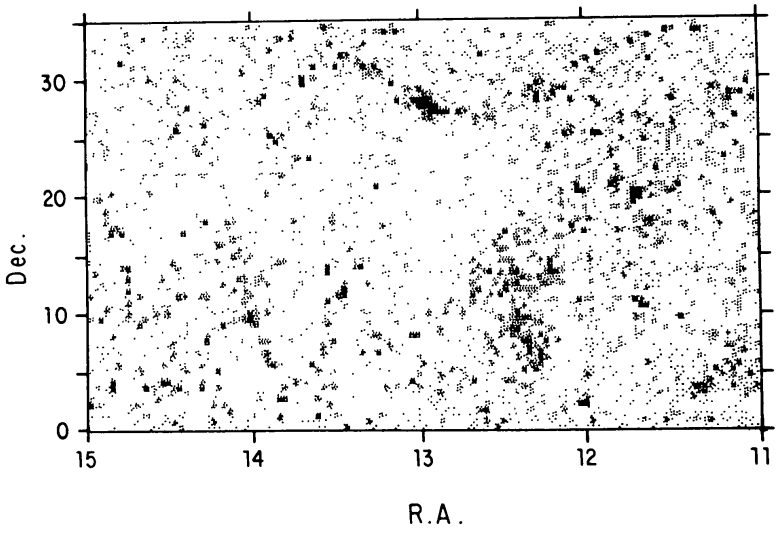

Figure 11 Distribution of galaxies in a large region containing the Coma supercluster [see (34) and text].

© Annual Reviews Inc. • Provided by the NASA Astrophysics Data System

1983ARA&A..21..3730

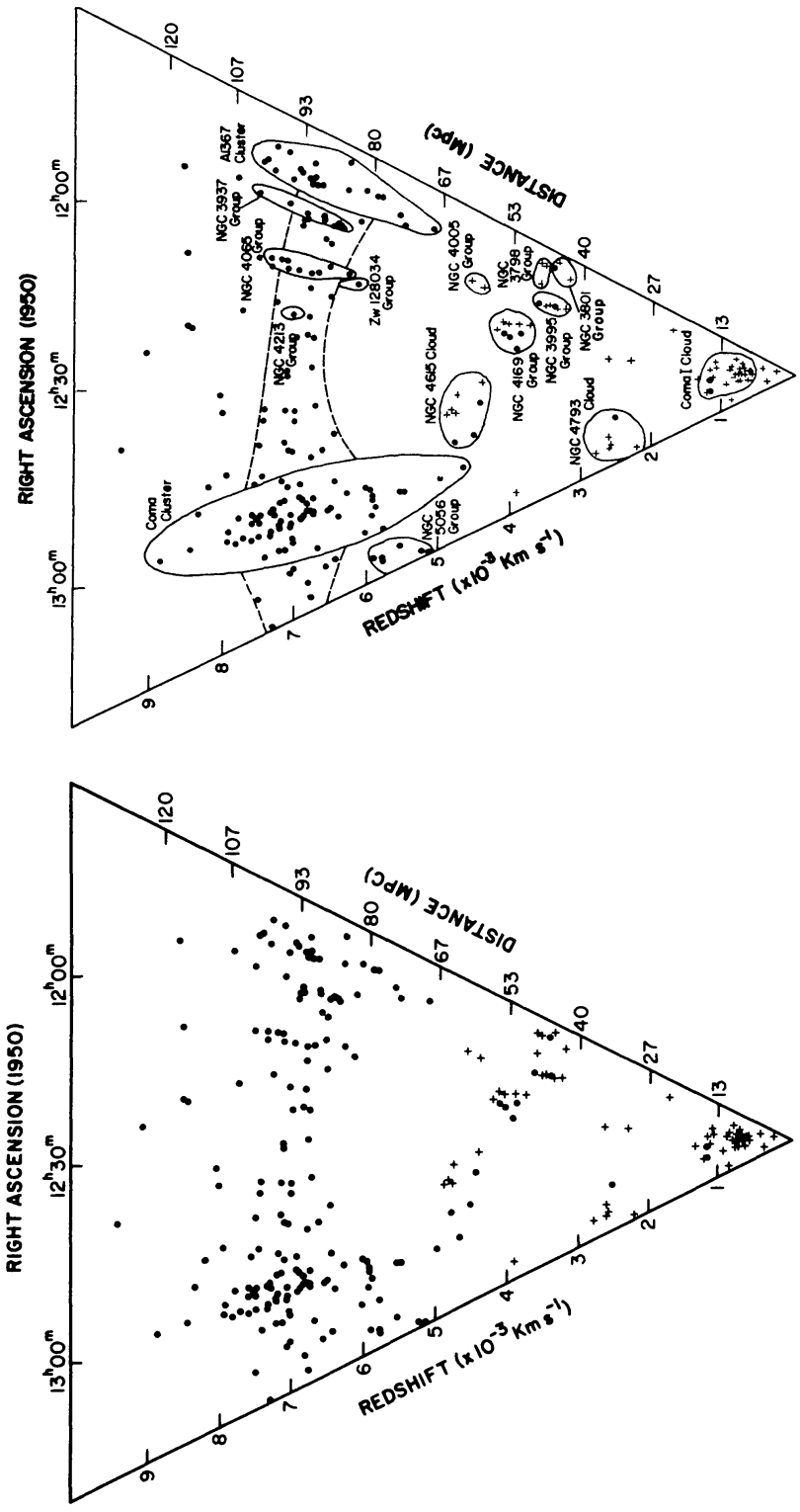

Figure 12 "Wedge diagram" of the Coma supercluster [Gregory & Thompson (40)]. As the supercluster is elongated in the east-west direction, right ascensions have been chosen as position coordinates; the galaxies lie between +19° and +32° declination. The angular size has been magnified about two times compared with the indicated distance scale.

© Annual Reviews Inc. • Provided by the NASA Astrophysics Data System

1983ARA&A..21..3730

NGC 5056 group (Zwicky 160-7) at $13^h20^m + 31°.6$, which is itself elongated in the same direction.

If the line-of-sight velocities are also representative for the random internal motions in the other coordinates, the "crossing" times exceed the age of the Universe, even along the short axis. For the long axis, they would exceed it by an order of magnitude. In this direction there cannot have been any appreciable mixing.

It is of interest to note that the northeastern end of the supercluster seems to point to the northern tip of the Hercules supercluster, which is indicated by a contour HER in Figures 9 and 10*b*. The Hercules supercluster extends from about $+15°$ to $+40°$ declination between right ascension $15^h.9$ and $16^h.5$ (see Section 6). Its velocity exceeds the 10,000 km s^{-1} limit of Davis et al.'s survey except at its northern end, where it is 9000 km s^{-1}; the nine galaxies in Figure 10*b* between α $16^h.0$ and $17^h.0$, and v 9000 and 10,000 km s^{-1} are therefore members of this supercluster, the main ridge of which extends in the north-south direction, almost at right angles to that of the Coma supercluster. The important question of whether the two superclusters are connected can only be decided when velocities for more galaxies in the gap between 14^h and 16^h have become available.

The Coma supercluster has been a subject of previous studies, in particular by Gregory & Thompson (40), who firmly established the existence of a bridge between the Coma and Abell 1367 clusters (Figure 12). The data show a second supercluster in front, at velocities between 3000 and 5000 km s^{-1}, and a nearby cloud which is not discussed here.

Their results agree very well with those of Davis et al.; the latter extend over a much larger area, and made it possible for the first time to determine the total length and width of both superclusters. In Gregory & Thompson's figure, various smaller groups are marked illustrating the clumpiness of the structure.

We can try to estimate the mass of the Coma supercluster on the uncertain hypothesis that the ratio between the number density of luminous galaxies and total mass density in the supercluster is the same as in the Universe.

Outside the supercluster the total number of galaxies with velocities between 6000 and 8000 km s^{-1} is about 217 in the north galactic polar cap and 93 in the south galactic polar cap. The areas are about 1.8 and 0.8 ster, yielding 121 and 116 galaxies per ster in the two regions, respectively. On the assumption that the galaxies lie in a shell with radii of 120 and 160 Mpc, the average density per 10^6 Mpc^3 is found to be 151.

There are 54 galaxies in the supercluster area itself, within an ellipse of $37° \times 11°$; subtraction of an estimated 12 "background" galaxies leaves 42 for the supercluster. As its volume is 0.033×10^6 Mpc^3 (if the line-of-sight

© Annual Reviews Inc. • Provided by the NASA Astrophysics Data System

1983ARA&A..21..3730

axis is assumed to be the same as the short axis on the sky), the density is 1290 per 10^6 Mpc^3, or 8.4 times the general average density derived above.

If the Universe has one tenth of the critical density, it has a density of 7.0 $M_\odot$ per kpc^3. The mass of the supercluster outside the two clusters is then 2×10^{15} $M_\odot$. The mass of the Coma cluster has been estimated at 4.7×10^{15} $M_\odot$ [N. Bahcall (5)]. That of Abell 1367 may be two or three times smaller; the combined mass of the two clusters would then be roughly three times that of the dispersed mass. The total mass of the supercluster is slightly less than 10^{16} $M_\odot$.

4.3 *Other Superclusters in the North Galactic Cap*

It is evident from Figures 8–10 that there are many more concentrations that have the characteristics of superclusters. By a simple inspection of Figure 8 one can outline at least half a dozen concentrations that are fairly isolated on the sky as well as in velocity. To illustrate the kind of "clouds" considered, three specimens have been indicated by contours marked SER (for Serpens), BOO 2, and BOO 3. They are similarly indicated in Figures 10*a,d*. In Figure 9 and the corresponding plots in Figure 10, some seven other isolated "clouds" can be seen beside Coma and Hercules. The richest one has been indicated as BOO 1 in Figures 9, 10*d*, and 10*e*.

Clearly, there is an arbitrariness in outlining these structures. They are also certainly incomplete. But they can serve to give an impression of the frequency of superclusters and their sizes.

The major diameters range from $\sim$12 to at least $\sim$90 Mpc. The dimensions are therefore the same as those found in the much deeper survey by Shane & Wirtanen (Section 2), but because of the radial-velocity data they are much better defined. The axial ratios vary from 0.2 to 0.9. The superclusters seen in Figure 8 cover approximately 0.48 ster, which is 25% of the total surface of the polar cap. Similarly, those in Figure 9 cover about 0.66 ster, or 35% of the surface surveyed. These numbers are for the velocity ranges 3000 to 6000 and 6000 to 10,000 km s^{-1}, respectively. They yield values for the average separation between superclusters along a line of sight of about 240 Mpc and 230 Mpc in the two shells. These values are about half as large as those quoted in earlier investigations [cf. Gregory et al. (41), Oort (60)] in which only the major superclusters were considered. The density of superclusters per 10^6 Mpc^3 is 9.4 in the first shell and 2.3 in the second. The relative smallness of the density in the second shell may be mainly due to the circumstance that many of the superclusters recognized in the nearer shell contain too few luminous galaxies, or are too small, to be identified in the almost two times more distant outer shell.

The determination of the mean separation between superclusters is of interest because it may be reflected in other phenomena, such as, for

© Annual Reviews Inc. • Provided by the NASA Astrophysics Data System

1983ARA&A..21..3730

instance, the mean separation in z between Lyman α absorption lines in quasars [cf. Sargent et al. (74), Oort (60)].

The preceding rough inventory of superclusters in Davis et al.'s survey also provides an indication of the extent to which galaxies are concentrated in superclusters. A rough estimate shows that in each of the two samples (Figures 8 and 9) 64% of the galaxies lie in well-isolated superclusters, while another 15% lie in less well-defined, but nevertheless probably genuine, agglomerations.

4.4 *The South Galactic Polar Cap*

Davis et al. have also surveyed a part of the south galactic polar cap, which is important for further detailed research on the superclustering phenomenon. But as the region covered is much smaller than that in the north, the survey does not lend itself so well for investigating the statistics of superclusters. It does, however, show that there is no great difference between the two polar caps, neither in character nor in general density.

4.5 *Regions Devoid of Galaxies*

Figures 8–10 not only contain a wealth of information on large concentrations of galaxies, but also equally interesting data on empty regions, as a simple inspection will make evident. These "holes" are often quite extended. Further discussions on voids are given in Sections 9.7 and 10.

5. THE PERSEUS SUPERCLUSTER

The investigations of Einasto and coworkers at Tartu [Einasto et al. (29), Jôeveer et al. (49)] further indicate the complexity of some of these superstructures. They investigated large-scale structures in the south galactic hemisphere above $-2°$ declination, using clusters from the catalogs of Zwicky et al. (101). Distances were derived partly from redshifts and partly from apparent magnitudes. The distribution in two redshift intervals is shown in Figure 13. Figure 14 gives the distribution of galaxies estimated to lie in approximately the same distance range as the clusters in Figure 13*a*. In both Figures 13*a* and 14 there is a concentration in an inclined ridge running from the Perseus cluster (Abell 426) to a region around 23^h3 $+25°$, and a less complete and wider band extending from Abell 426 (in the upper left) to Abell 194 at the bottom of the picture. In the range 6500–10,000 km s^{-1} these ridges have disappeared. The two ridges are considered by the authors to be parts of a large supercluster, which comprises also the group around Uppsala 487 in the lower right. It covers about 1600 square degrees, or 5000 Mpc^2. The densest region is the chain in the northern part, which contains three Abell clusters as well as the NGC

© Annual Reviews Inc. • Provided by the NASA Astrophysics Data System

1983ARA&A..21..3730

383 and NGC 507 clusters. A more recent investigation by Gregory et al. (41) has confirmed that the galaxies in this chain have velocities that are strongly concentrated around a mean of 5165 km s^{-1}. The dispersion is 442 km s^{-1} (cf. Figure 15). The dispersion on the plane of the sky, perpendicular to the direction of the chain, is given as 5°.6 by Gregory et al., a value corresponding to 10 Mpc on our distance scale, but it is only half this in the western half of the chain, between $0^h.0$ and $1^h.8$; the axial ratio is about 5:1. New velocity measurements by Focardi et al. (33) confirm that the chain extends westward to 23^h55^m. The total length of the ridge is 75 Mpc.

The Perseus cluster itself seems to contain a stringlike arrangement of bright galaxies, which Rood & Sastry (68), in their classification scheme of clusters, reproduced as an illustration of a "line cluster" [cf. Struble & Rood (86)]. It may be noted that the position angle of this 1.0-Mpc "string" coincides within 4° with that of the 70-Mpc northern ridge of the supercluster. Considering the mixing time in the cluster, the reality of the small string is somewhat doubtful.

A comprehensive study of the entire supercluster was made by Giovanelli et al. (39). They combined velocity data from the Harvard Center for Astrophysics with about 1100 21-cm redshifts, which they measured with the Arecibo 305-m telescope. Well over half of the more than 1400 velocities measured in the entire area of $6^h \times 40°$ are sharply peaked near 5000 km s^{-1}, showing that the majority of all galaxies measured belong to one structure extending over more than 2000 square degrees. The authors remark that the detailed structure "appears as a maze of thin filamentary structures. . . . Unbroken . . . segments can extend for several tens of Mpc along one dimension, while they are very thin in the other two, with axial ratios usually larger than 10." The total mass is estimated as $10^{16-17}\,\Omega\,M_\odot$ [Giovanelli (37)]. Einasto has given a value of $2.8 \times 10^{16}\,M_\odot$.

Giovanelli et al. (39) also report on an important new property. They plotted the galaxies separately for different galaxy types, and found that the main ridge is considerably narrower and stands out much clearer in the early types than in the later types. There is a regular progression of this property from E/S0 to Sc and Irr as shown in Figure 16. The last three panels give all galaxies listed in the Uppsala catalog for which radial velocities were known at the time when the diagrams were made. The panels show the distributions for E-S0-Sab, Sb-Sbc, and Sc-Irr and dwarfs. As there were relatively few radial velocities for the early types, I have added in the upper-left panel the distribution of all E-S0,a galaxies, whether or not their velocities were known. There appears to be a rather striking progression with galaxy type in the sharpness of the branches of the supercluster. Differences of the same nature have long been known to exist in clusters, but this is the first evidence for such a segregation in an

© Annual Reviews Inc. • Provided by the NASA Astrophysics Data System

1983ARA&A..21..3730

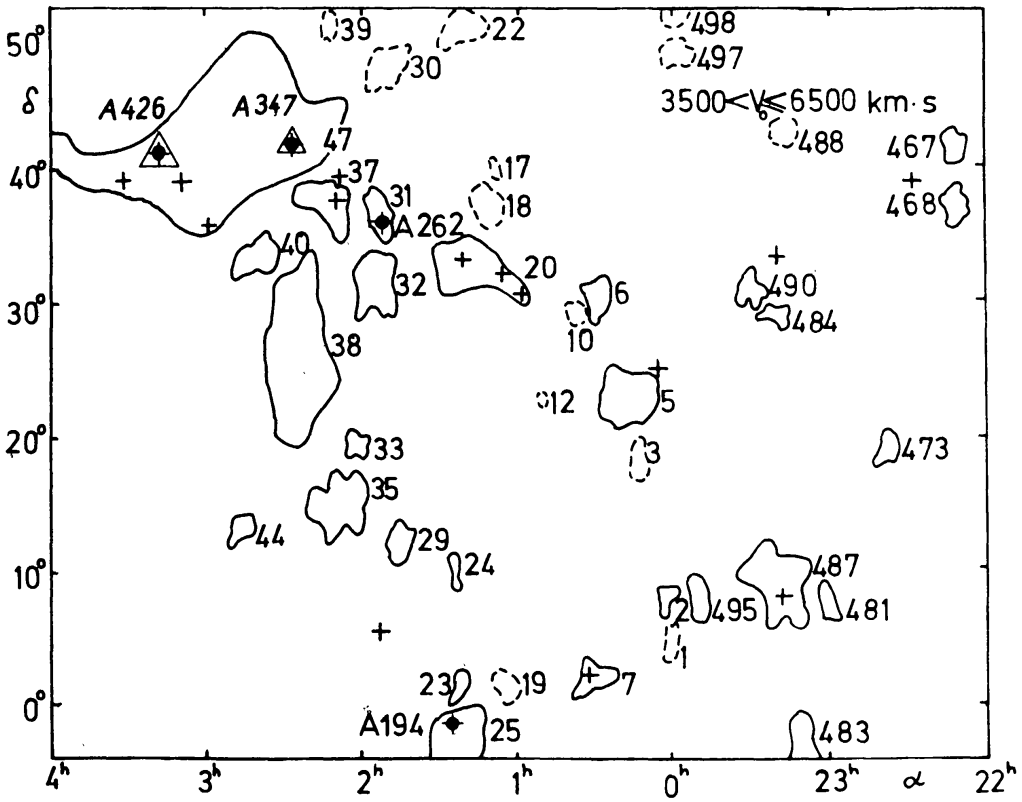

(a)

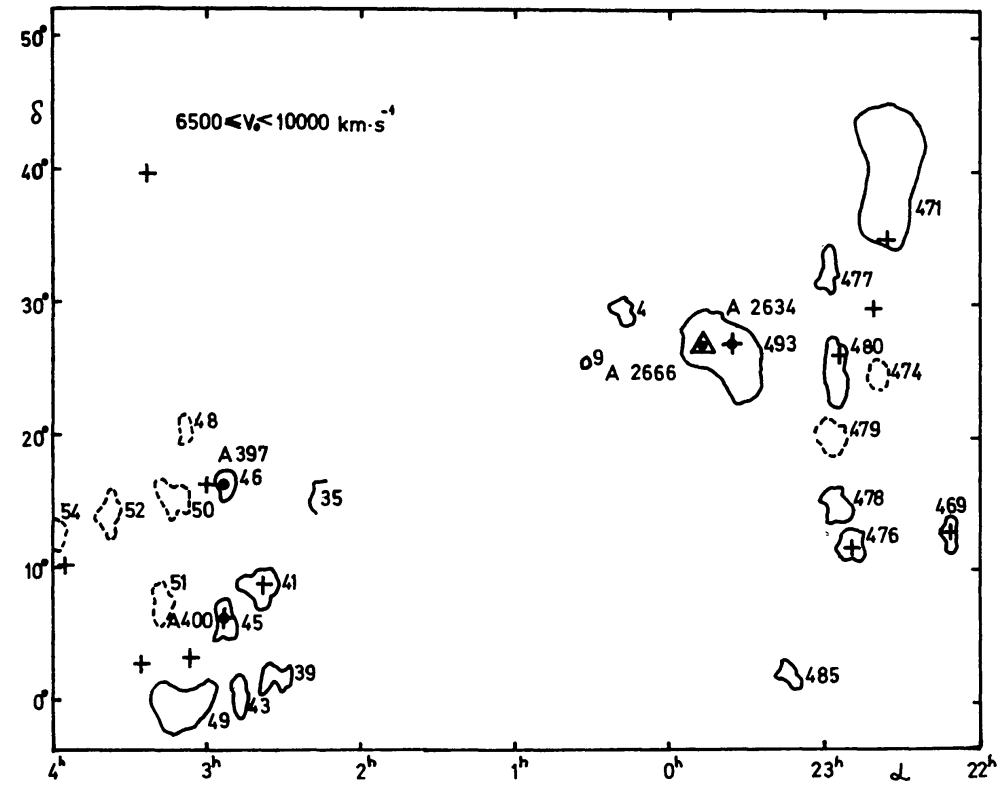

(b)

© Annual Reviews Inc. • Provided by the NASA Astrophysics Data System

1983ARA&A..21..3730

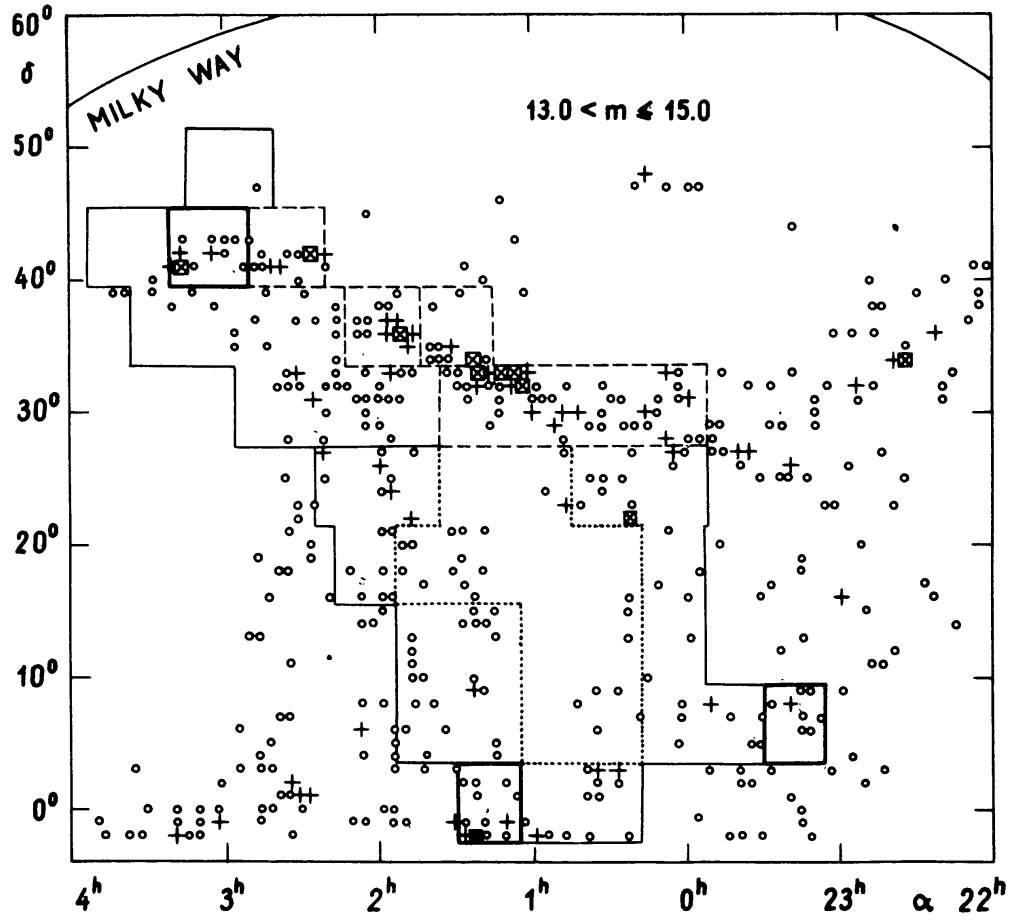

Figure 14 Perseus supercluster. Distribution of galaxies between $13^m.0$ and $15^m.0$ in the same region as that shown in Figure 13*a*. Symbols indicate numbers per square degree (circles 2–3, crosses 4–7, crosses in squares 8–15) [from Einasto et al. (29)].

unrelaxed and thinly populated feature. It indicates that galaxies were born in the supercluster, which thus must have been gaseous; the E and S0 galaxies have apparently formed in the dense inner part of the "filament," with the spirals forming from gas falling in later (cf. Section 10 for a further discussion).

An interesting further property of the supercluster is that the major axes of the rich clusters Abell 426, 347, and 262 are oriented within 10°–20°

Figure 13 Perseus supercluster. The distribution of Zwicky clusters with velocities between 3500 and 6500 km s^{-1} (*a*), and between 6500 and 10,000 km s^{-1} (*b*) in the south galactic hemisphere. Solid contours show the clusters with measured redshifts, dotted contours indicate those with distances estimated from magnitudes and cluster diameters. The numbering is from Nilson (57). Abell clusters are indicated by solid circles and by their numbers in Abell's catalog (2); A 426 is the Perseus cluster. △: (X-ray sources), +: (radio sources). [Reprinted by courtesy of Einasto et al. (29).]

© Annual Reviews Inc. • Provided by the NASA Astrophysics Data System

1983ARA&A..21..3730

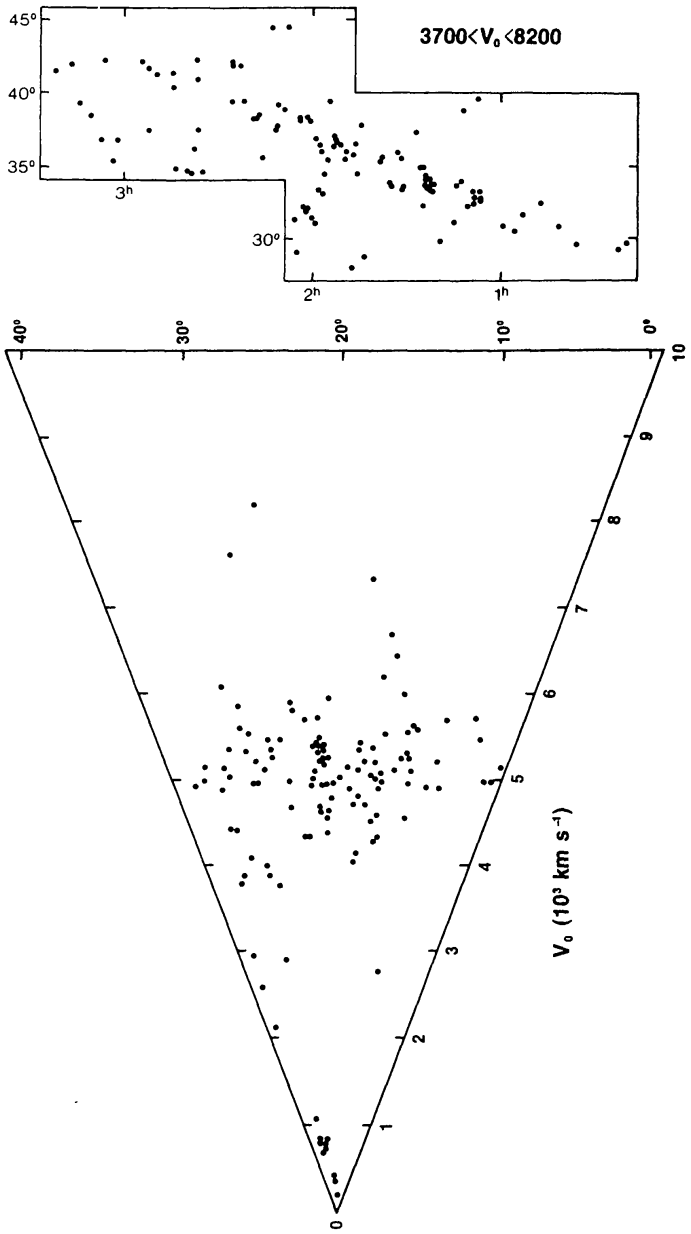

Figure 15 Perseus supercluster. (*Top*) Distribution of galaxies brighter than $m_p = 14.0$ in the Zwicky catalogue and having velocities between 3700 and 8200 km s^{-1}. The boundaries of the region surveyed are indicated. The tips of the Perseus supercluster chain lie around $\ell = 150°$, $b = -12°$ (*left*) and $\ell = 115°$, $b = -34°$ (*right*); (*Bottom*) "Wedge" diagram for all galaxies in the survey with velocities less than 10,000 km s^{-1}. The positions are measured along the chain [from Gregory et al. (41)].

© Annual Reviews Inc. • Provided by the NASA Astrophysics Data System

1983ARA&A..21..3730

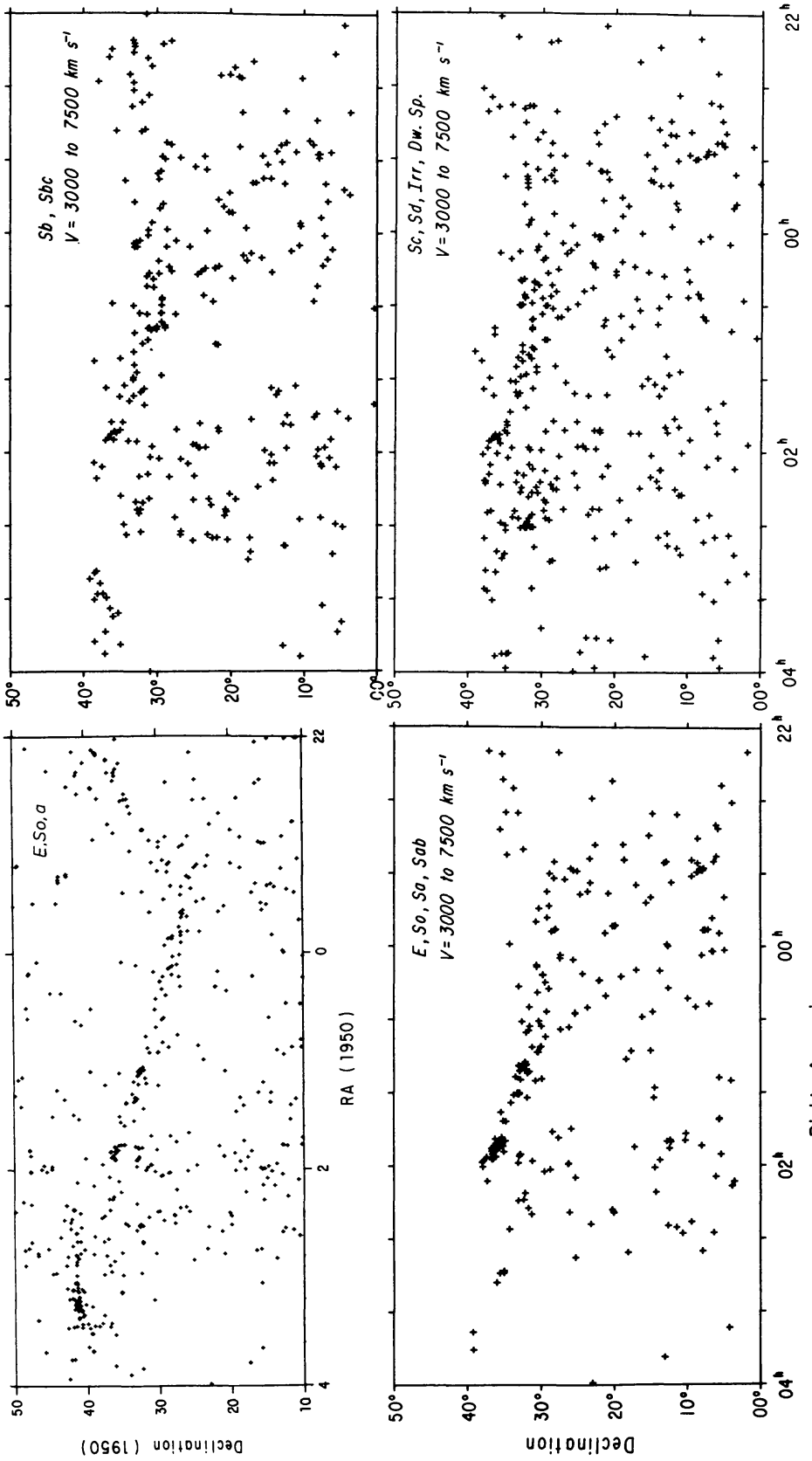

Figure 16 Distribution of galaxies from the catalog by Zwicky et al. (101) in the region of the Perseus supercluster. (*Top left*) E-S0,a for all velocities; the other panels are limited to galaxies with velocities between 3000 and 7500 km s^{-1} [Giovanelli et al. (39)]. I am greatly indebted to the authors for putting their most recent material at my disposal in advance of publication.

© Annual Reviews Inc. • Provided by the NASA Astrophysics Data System

1983ARA&A..21..3730

of the direction of the main ridge (29, p. 366). Similarly, the major axis of Abell 194 in the south is directed toward the Perseus cluster Abell 426. This property is further discussed in Section 9.5.

Burns & Owen (12) have suggested on the basis of the distribution of radio galaxies with velocities between 4810 and 6300 km s^{-1} that the Perseus supercluster might extend across the Milky Way, and include Abell 569 at $7^h04^m +48°$, $v = 5800$ km s^{-1}. This lies 4^h east of the Perseus cluster. An extension across the zone of avoidance has likewise been suggested by Giovanelli & Haynes (38). They point to a possible connection with a long chain in Lynx and Ursa Major at a velocity of 4200 km s^{-1}. The evidence for these suggested connections is still very uncertain.

In the large region investigated by Einasto et al. (29), three other important superclusters are defined by the authors. They also draw some general conclusions about the nature of superclusters. They believe that neighboring superclusters are in contact and form walls and ribs of "cells"; as stated by the authors, "the space inside the cells is void of clusters and almost void of galaxies." They believe, furthermore, that all galaxy clusters and most other galaxies are located in superclusters.

6. THE HERCULES SUPERCLUSTER

A fourth large superstructure for which a fair amount of data is available is that in Hercules. It contains two groups of rich clusters, one near Abell 2151 (the Hercules cluster), with a velocity of 11,000 km s^{-1}, and the other near Abell 2199 at a velocity of 9000 km s^{-1}. As early as 1934, Shapley (82) had called attention to the first group, which he called the "double supergalaxy in Hercules." Abell (3) suggested that the two groups, separated by 25° (corresponding to 89 Mpc), are part of the same supercluster. Direct evidence of a bridge of galaxies connecting the two main groups has been produced by Chincarini et al. (15), and is shown in Figure 17. They determined redshifts for a sample of 44 galaxies with Zwicky magnitude brighter than 15.8 in the area between the two groups. As these are mainly separated in declination, the velocities are plotted against declination. The velocity dispersion of the bridge is found to be ~ 800 km s^{-1}.

In front of the bridge there appears to be a void between 7000 and 8500 km s^{-1}. A somewhat larger, and better established, void had already been found in the region from $+14°$ to $+22°$ declination, in which a large number of velocities had been determined by Tarenghi et al. [(89); cf. Figure 18]. Here the hole extends from 5300 to ~ 9000 km s^{-1}. There is a second supercluster at $v = 4800$ km s^{-1}.

Observations by Tarenghi et al. (88) have indicated that the Hercules

© Annual Reviews Inc. • Provided by the NASA Astrophysics Data System

1983ARA&A..21..3730

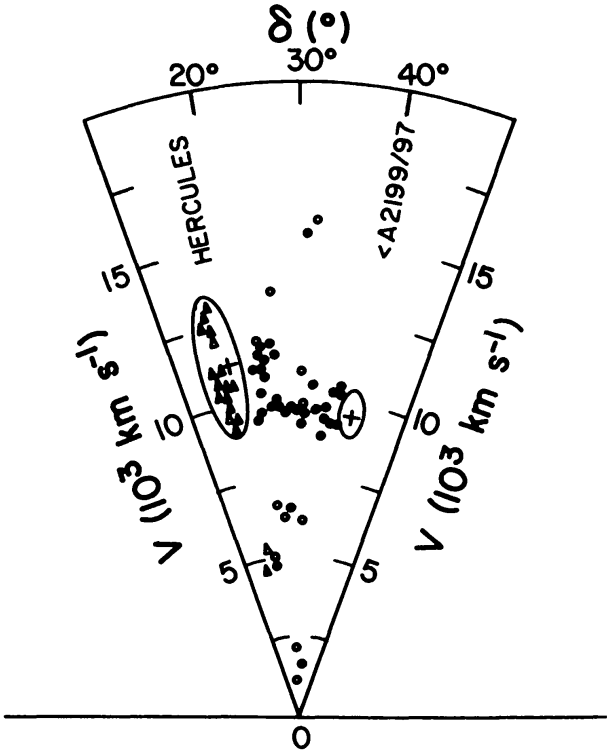

Figure 17 The Hercules supercluster. Radial velocities of galaxies between the two principal groups of clusters (which have been indicated by elliptical contours) plotted against declination. Data for Hercules (*triangles*) are from Tarenghi et al. (88, 89); the ellipse for A 2199/A 2197 is from Thompson & Gregory (90). Reproduced by kind permission of Chincarini et al. (15) and the *Astrophysical Journal.*

supercluster probably extends beyond Abell 2197 to a declination of 55° (cf. Figure 19). It then would span an arc of at least 40°, and would have a length of 143 Mpc.

Burns & Owen (12) have suggested a possible further extension toward low declinations (down to $\delta = +7°$), which would include two radio galaxies with velocities in the appropriate range, and the clusters Abell 2063 and 2052 at velocities of 10,100 and 10,400 km s^{-1}.

Only fragmentary data are available about the distribution on the sky [cf. (89) for the part between $\delta = 15°$ and 22°; (15) for the bridge]. The six Abell clusters in the two groups lie practically on a line; Abell 2146, which is about midway between the two compact groups, deviates less than a degree from this line, while its velocity differs by only 400 km s^{-1} from that interpolated between the two groups; the velocity is not very accurate. The galaxies spread over a wider region than the clusters; their distribution appears to be irregular, with a width in right ascension between 10° and 15°.

© Annual Reviews Inc. • Provided by the NASA Astrophysics Data System

1983ARA&A..21..3730

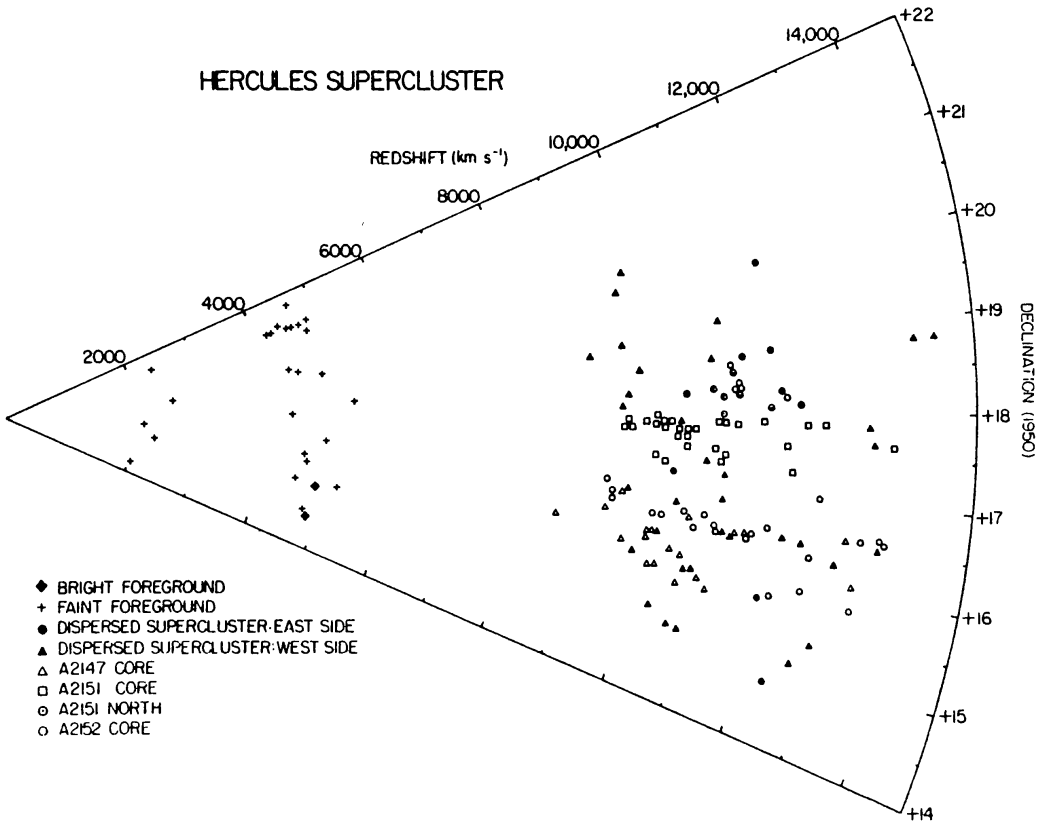

Figure 18 The Hercules supercluster (southern part). Reproduced by kind permission of Tarenghi et al. (89) and the *Astrophysical Journal.*

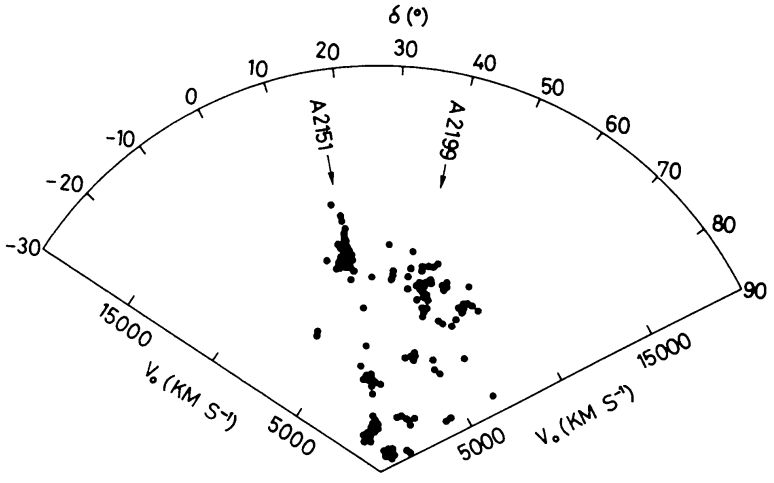

Figure 19 The Hercules supercluster. "Cone diagram" of velocity versus declination for galaxies between 15^h30^m and 17^h0^m right ascension. Reprinted by courtesy of Tarenghi et al. (88) and the *Astrophysical Journal.*

© Annual Reviews Inc. • Provided by the NASA Astrophysics Data System

1983ARA&A..21..3730

7. SUPERSTRUCTURES OF RICH CLUSTERS

Valuable information on superclustering in a large volume of space is furnished by the surveys of clusters of galaxies. There are two large catalogs: Zwicky et al.'s *Catalogue of Galaxies and Clusters of Galaxies* (101), comprising some 20,000 clusters, and the catalog of rich clusters by Abell (2), which contains 2712 clusters. Both rest on surveys of the plates of the National Geographic Society–Palomar Observatory Sky Survey. Zwicky et al. (101) list clusters and groups of greatly varying sizes, the contours being defined as the isopleths where the surface density of galaxies is about twice that of neighboring fields. Abell used a more exacting criterion: there should be at least 50 members within a circle of radius 3 Mpc (on the $H = 50$ scale). Moreover, he selected a sample of 1682 clusters which he considered as a homogeneous sample; this covers the sky north of declination $-27°$ and avoids lower-latitude regions of strong absorption. His catalog of rich clusters gives rough indications of richness and distance. He distinguished six distance groups, as indicated in Table 1, in which the distances are based on a Hubble constant of 50 km s^{-1} Mpc^{-1}. Abell is preparing an extension of his catalog to the south pole, using the deep survey made with the Anglo-Australian Schmidt telescope.

A proper search for superclusters in the rich material contained in the two cluster surveys must await the determination of radial velocities.[2] But even without these, some information can already be extracted. The following discussion is mainly restricted to the more or less homogeneous material of Abell's catalog.

As may be seen in Figure 20, the distribution of the clusters is strikingly uneven, with agglomerations of various sizes. Abell (3) has made an extensive study of this clumpiness. He divided the sky into equal-size cells,

Table 1 Mean distances of clusters in Abell's distance groups

Distance group (D)	Mean distance (Mpc)
1	160
2	230
3	400
4	540
5	840
6	1080

[2] A table of redshifts for Abell clusters has been given by Sarazin et al. (73); it contains 329 clusters, including those in a recent table by Hoessel et al. (44). Extensive additional data are given by Fetisova (31). Schneider et al. (77a) have determined velocities for 84 Abell clusters.

© Annual Reviews Inc. • Provided by the NASA Astrophysics Data System

1983ARA&A..21..3730

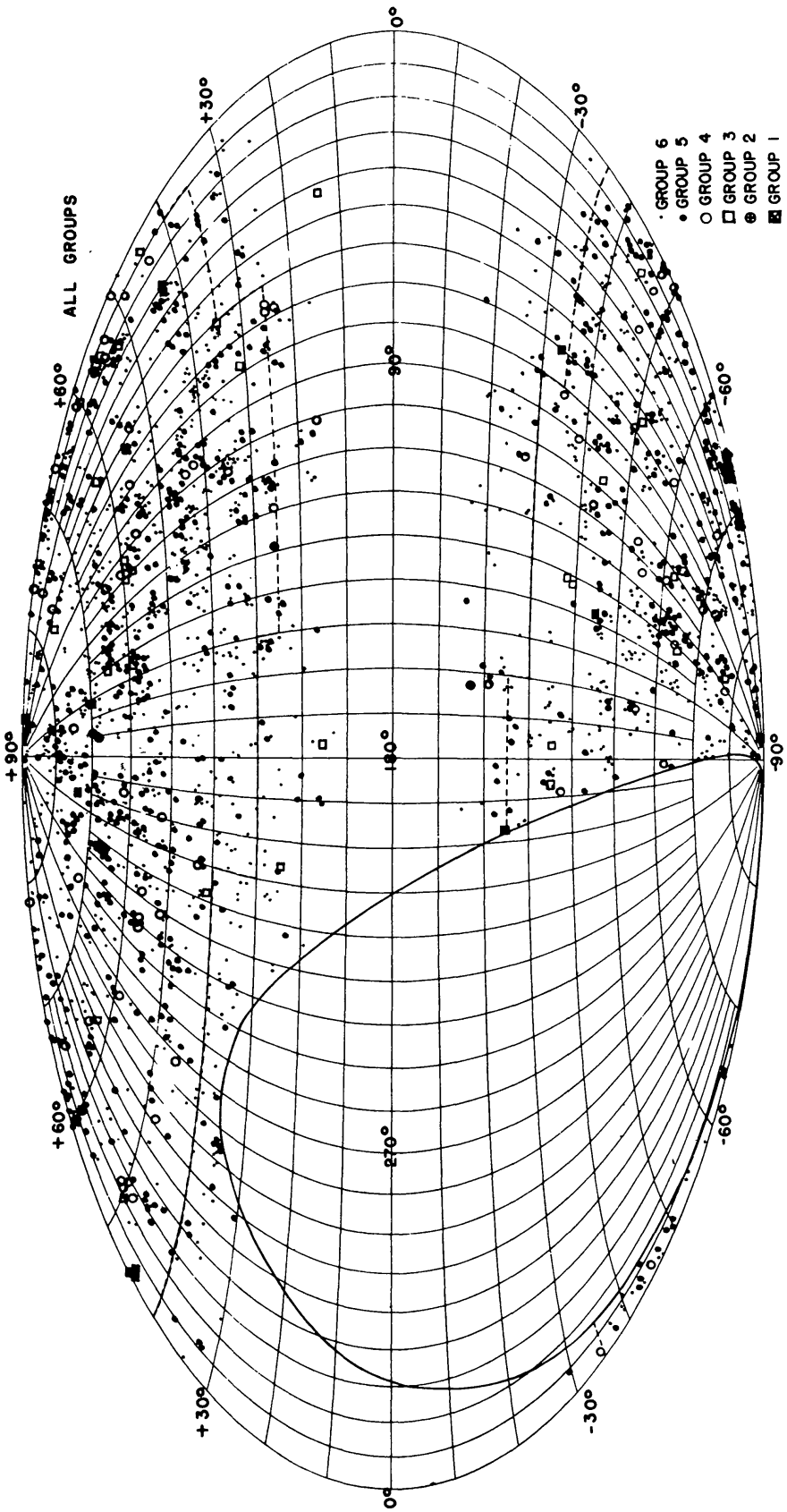

Figure 20 Distribution of galaxy clusters in Abell's catalog. The coordinates in the Aitoff equal-area projection are galactic longitudes and latitudes on the old system; new galactic longitudes are 32° higher. The large empty oval region is the part of the sky not covered by the Palomar Sky Survey. The distance groups are indicated by different signs. Reproduced by courtesy of G. O. Abell (3).

© Annual Reviews Inc. • Provided by the NASA Astrophysics Data System

1983ARA&A..21..3730

and found that maximum deviations from a random distribution occur when the diameters of the fields are taken to be 5° in his more distant group, and proportionally larger in the nearer groups. The corresponding linear size is 90 Mpc. Similar dimensions were found by Hauser & Peebles (43) from a correlation analysis, which gave a "clustering length" $r_s \simeq 60$ Mpc.

Abell (3) listed 17 of what he called "second-order clusters," with an average membership of 11. A further list of 21 possible superclusters was extracted from Abell's catalog by Murray et al. (55). Confirmation of the physical reality of these agglomerations must await the observation of radial velocities.

Recently, N. Bahcall & Soneira (8) made a new analysis of the correlation function of Abell clusters. They used a complete sample of 104 clusters of distance class $D \leq 4$ and richness class >0, for all of which radial velocities had been measured. They found that the function $\xi(r) = 1250\ r^{-1.8}$ (for $H_0 = 50$ km s^{-1} Mpc^{-1}) well represented the data up to $r \simeq 300$ Mpc; the correlation scale length was 50 Mpc, about five times larger than that for galaxies. The authors also found that this length increases strongly with the richness of the clusters; in combination with the galaxy-galaxy correlation functions, this indicates that "progressively stronger correlations exist for richer galaxy systems." These conclusions were tested and verified against a deeper and larger sample of 1547 distance-class 5 and 6 clusters for which no velocities were available.

It is remarkable that the correlation function for the clusters has the same form as that for the galaxies, but with a five times larger scale length.

There is considerable evidence for larger agglomerations, some of which (such as the one in Hercules) have been discussed in previous sections. N. Bahcall & Soneira (9) made a systematic search in their sample of 104 clusters. They give a list of 16 superclusters satisfying certain strict definitions of volume density enhancement. The distribution in the north galactic hemisphere is shown in Figure 21, which may be considered as a complete map of giant superclusters to a distance of ~ 500 Mpc. The numbers refer to the authors' list made on the basis of the contours indicating a minimum space density enhancement factor of 20. Higher density contours are also shown. The three most important features are 15 and 16 (Hercules, 7 rich clusters—diam. 145 Mpc); 12 (15 rich clusters, among which is the Corona Borealis cluster—diam. 360 Mpc); and 8 (5 rich clusters, among which is the Ursa Major cluster—diam. 80 Mpc). The two Hercules clumps are joined together when clusters of richness class 0 are added. The authors noted that several of their superclusters coincide with rather striking structures in the Shane-Wirtanen galaxy survey (80) as depicted in Figure 3 of (85) (N. Bahcall, private communication).

Just like galaxies, clusters also have a tendency for clumping in smaller

© Annual Reviews Inc. • Provided by the NASA Astrophysics Data System

1983ARA&A..21..3730

groups. A number of such groups, with diameters generally less than ~25 Mpc, have been identified by Rood (67).

Ford et al. (35) have recently measured radial velocities in three other second-order clusters. In one case, there appeared to be no coherent association. In the other two, the reality of the groups was fully confirmed. These are 1451+22 = Abell No. 11 = No. 18 of the list by Murray et al. (55), and 1615+43 = No. 19 of Murray et al. They lie beyond the distance limit of Figure 21 (at 700 and 810 Mpc) and contain 7 and 6 rich clusters,

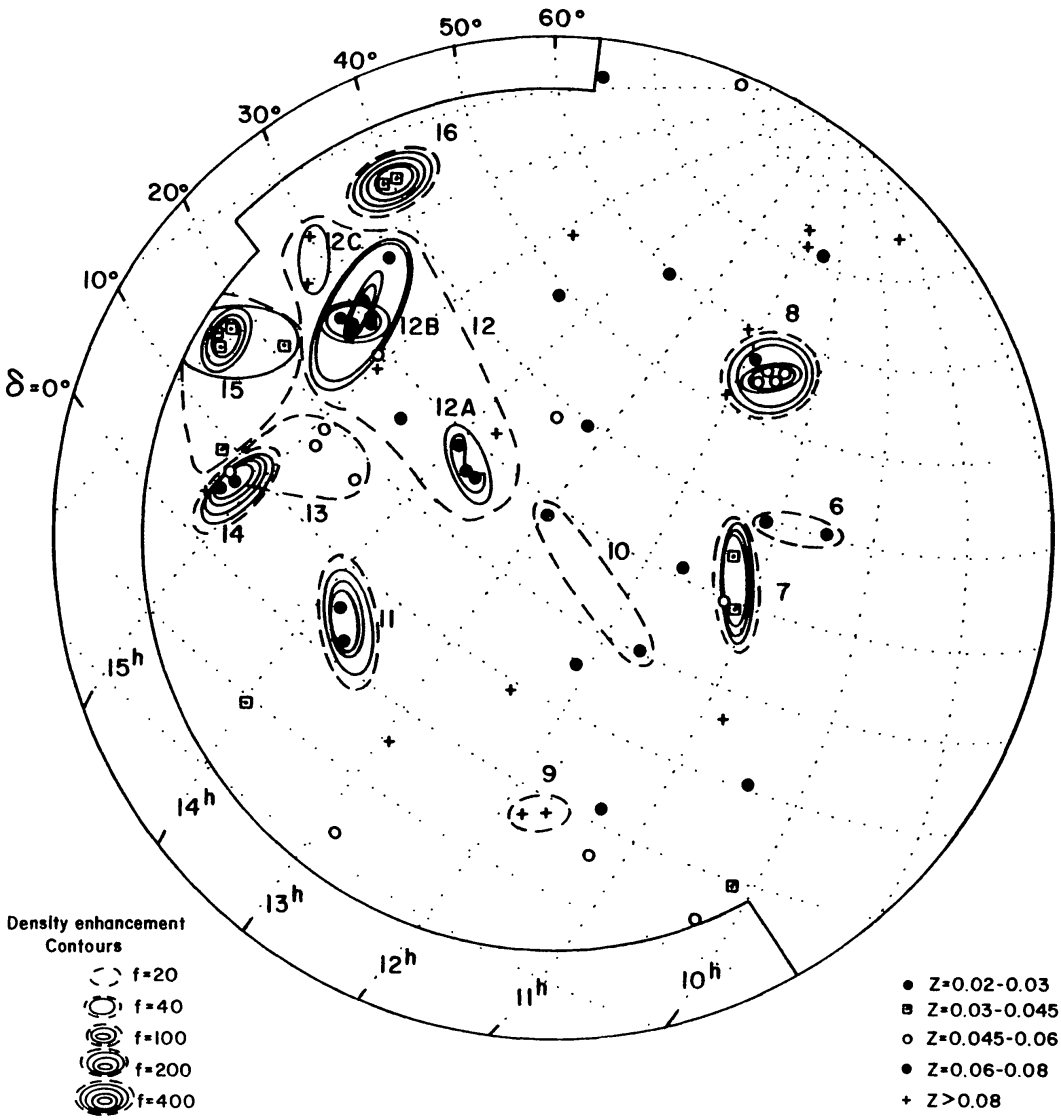

Figure 21 Giant superclusters in the north galactic hemisphere above 30° latitude. The outermost contour is $b = 30°$; the inner contour is the completeness limit of the sample. Small contours show the space density enhancement factor over the mean space density at the distance of the supercluster. Numbers refer to the authors' list of superclusters. The elongated contour number 10 is the Coma supercluster. Reproduced by courtesy of N. Bahcall & Soneira (9).

© Annual Reviews Inc. • Provided by the NASA Astrophysics Data System

1983ARA&A..21..3730

respectively; redshifts were measured for all 13 of these clusters, as well as for 19 groups and poor clusters, of which 15 proved to be members. The superclusters are elongated, with major diameters of roughly 100 Mpc (Figure 22). The velocity distributions are shown in the lower part of the figure; dispersions are 478 and 720 km s^{-1}, respectively.

Knowledge about clusters south of the region covered by Abell's survey is scarce. There is an exceptionally rich field in and around the constellation Horologium, which was covered by a Harvard survey [Shapley (83)]. Redshifts were recently determined in part of this field; they indicated the existence of a supercluster at 360 Mpc, containing at least two very rich clusters. There is also a large foreground structure at 270 Mpc distance [Lucey et al. (52)].

A question that naturally arises is whether density fluctuations exist on a much larger scale than the 100–200 Mpc typical for the largest superclusters found so far. Abell (3) experimented with cell sizes up to ~200 Mpc, where he still found a considerable deviation from a Poisson distribution. No clear evidence for inhomogeneity remains, however, when one goes to scales of the order of 1000 Mpc by comparing the numbers of distant clusters in

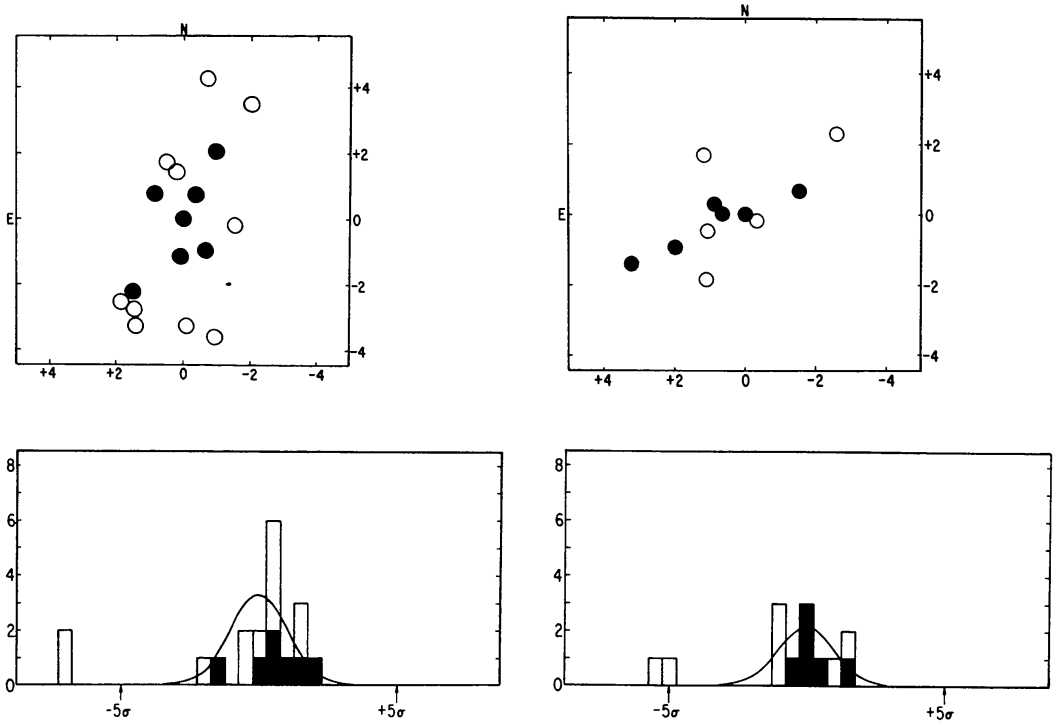

Figure 22 Sky (*top*) and velocity distribution (*bottom*) of two second-order clusters. Solid circles and rectangles are rich clusters, open circles and rectangles are groups and poor clusters. Bins in bottom figures have width of the velocity dispersion σ. Nonmember galaxies closest in velocity to that of the supercluster are also shown. Reproduced by courtesy of Ford et al. (35) and the *Astrophysical Journal*.

© Annual Reviews Inc. • Provided by the NASA Astrophysics Data System

1983ARA&A..21..3730

entire octants of the sky. A similar conclusion for a somewhat smaller scale had been reached in (46) from counts of individual galaxies. The problem is discussed further in the next section.

8. SUPERCLUSTERS AT LARGE REDSHIFTS; INHOMOGENEITY ON LARGEST OBSERVABLE SCALES

Because quasars can be observed to greater distances than other objects, they may enable us to find whether superclusters exist at much larger redshifts than have hitherto been surveyed. In quasar surveys, a supercluster might be discovered if it contains two (or more) quasars within the magnitude limit of the survey. Quasars lying in the same supercluster should have velocities differing by less than the velocity spread within a supercluster. We should therefore look for neighboring quasars with nearly equal redshifts. A number of fields of approximately one-degree diameter have been searched for faint quasars by Arp and collaborators (4). On the basis of recent data, there are three pairs of quasars in these fields with redshift differences of less than ~ 400 km s^{-1}; the separations on the sky are between 2 and 27 Mpc (reduced to $H = 50$) [cf. Oort et al. (61)].

The probability that the three pairs are chance coincidences was considered to be small, but there is doubt about the reliability of this conclusion on the ground that it was in part based on a posteriori probabilities. A larger set of data is required to obtain certainty. Half a dozen additional pairs, whose reality was judged to be probable, were found from surveys covering larger areas. Their separations range from 22 to 52 Mpc. Two of these have z values around 3, indicating that superclusters containing quasars might exist at an epoch when the age of the Universe was only one fifth of its present age.

An especially interesting case is that of a triple of quasars at $z = 2.05$ near M82, discussed by E. M. Burbidge et al. (11a). The three quasars lie within a circle of 1′.8, or 0.1 Mpc, radius and have redshifts of 2.048, 2.054, and 2.040, respectively. The probability that these quasars would accidentally lie so close together in space is so small that they must be considered as being physically connected. They show that clusters existed as early as $z = 2.05$.

An interesting *super*cluster, containing four quasars, was found at $z = 0.37$ (distance 2200 Mpc). It has a diameter of ~ 140 Mpc [(61), Webster (93a)].

It would, of course, be exceedingly interesting to investigate whether there exist any large-scale density variations in the distribution of quasars and radio galaxies. At present, no homogeneous surveys of quasars exist, but a more or less homogeneous survey of radio sources in general is

© Annual Reviews Inc. • Provided by the NASA Astrophysics Data System

1983ARA&A..21..3730

provided by the *Cambridge 4C Catalogue*. Clustering properties of sources in this catalog have been investigated by Seldner & Peebles (78), but no definite conclusion has resulted (probably due to the large spread in radio luminosity), except that any large-scale unevenness, if it exists, cannot be more than about 1%. A successful investigation may have to wait until wholesale redshifts are available.

Longair (51) has reviewed the evidence from other radio source catalogs; he concluded that there is no evidence for deviations from randomness in the distribution of the sources on the sky. From a discussion of the Bologna B2 catalog, Webster (93) has derived a limit $<3\%$ for the fluctuations on a scale of 1 Gpc. For a further discussion of the problem of very-large-scale clustering, see (64).

Evidence for homogeneity on the largest observable scale has come from measurements of the cosmic background radiation. It seems that the deviations from isotropy in this radiation can entirely be explained as coming from the motion of the Local Group relative to the surrounding Universe. Recent measurements at a wavelength of 1.2 cm have not confirmed the quadrupole effect, which had been indicated by earlier observations. An upper limit $\delta T/T \sim 5 \times 10^{-5}$ was derived. For an extensive discussion, see Wilkinson (95).

9. PROPERTIES OF SUPERCLUSTERS

9.1 *An Objective Measure of Superclustering*

Superclustering often appears in elongated, sometimes filamentary, and always extensive structures. In order to measure the strength of superclustering, or the "geometry" of the galaxy distribution, one should therefore devise a procedure that preferentially selects structures of this sort.

An interesting method, referred to as "cluster analysis," has been described and applied by Zeldovich et al. (99) [cf. also Einasto et al. (30)]. Similar procedures have been used in the percolation theory of the conductivity of semiconductors, among others. Briefly, the method works as follows: Consider a material of galaxies with known space coordinates. Draw a sphere of radius r around each galaxy. If this "neighborhood radius" r is small, the spheres will be "well separated from each other as 'islands' in a continuous 'ocean' of empty space. When we take a larger radius, a number of neighboring 'islands' join each other to form connected systems of galaxies. Using a still larger radius, most of the galaxies join to form large connected systems. At a very large radius practically all galaxies join to a single connected system" [quoted in essence from (99)].

In the articles cited, the basic observational catalog was centered on the

© Annual Reviews Inc. • Provided by the NASA Astrophysics Data System

1983ARA&A..21..3730

Virgo cluster and extended about 80 Mpc on either side in all three coordinates. Only galaxies brighter than $M_0 = -19.5$ were used. The data were based on a compilation of redshifts by Huchra; the total number of galaxies was 866.

The geometry of this observed catalog (O) is compared with that of three artificially constructed catalogs in Figures 23 and 24; model H was calculated from the hierarchical model of Soneira & Peebles (85), model P from a fully random (Poisson) distribution, while model A was taken from an N-body experiment based on the adiabatic scenario of structure formation proposed by Zeldovich and the Moscow school. All catalogs had roughly equal numbers and densities.

Figure 23 gives the maximum length of connected regions as a function of the neighborhood radius. It illustrates the good agreement of the A and O catalogs, and the entirely different behavior of P and H. The difference between H and O begins between $r = 1$ and 2 Mpc, corresponding to the transition from single to multiple clusters and chains. At $r \sim 5$ Mpc, the maximal length for O and A exceeds the size of the region studied.

Equally large differences between O and A on the one hand and P and H on the other are shown in Figure 24, which gives the distribution of the "multiplicities" (defined as the number of galaxies in connected systems in percentages of the total number of galaxies in the catalog). They were determined for a neighborhood radius $r = 5$ Mpc. The abscissae give the

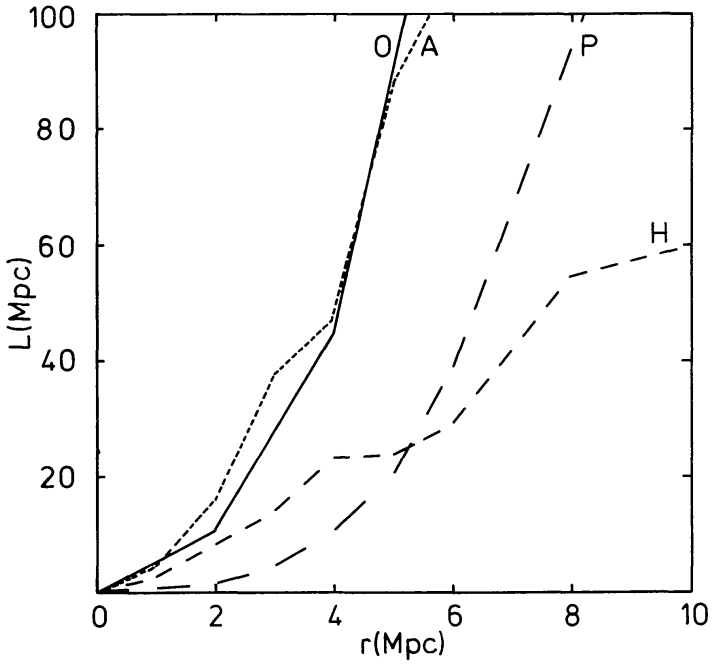

Figure 23 Maximal length of connected regions as a function of neighborhood radius r for four catalogs [courtesy of Zeldovich et al. (99)].

© Annual Reviews Inc. • Provided by the NASA Astrophysics Data System

1983ARA&A..21..3730

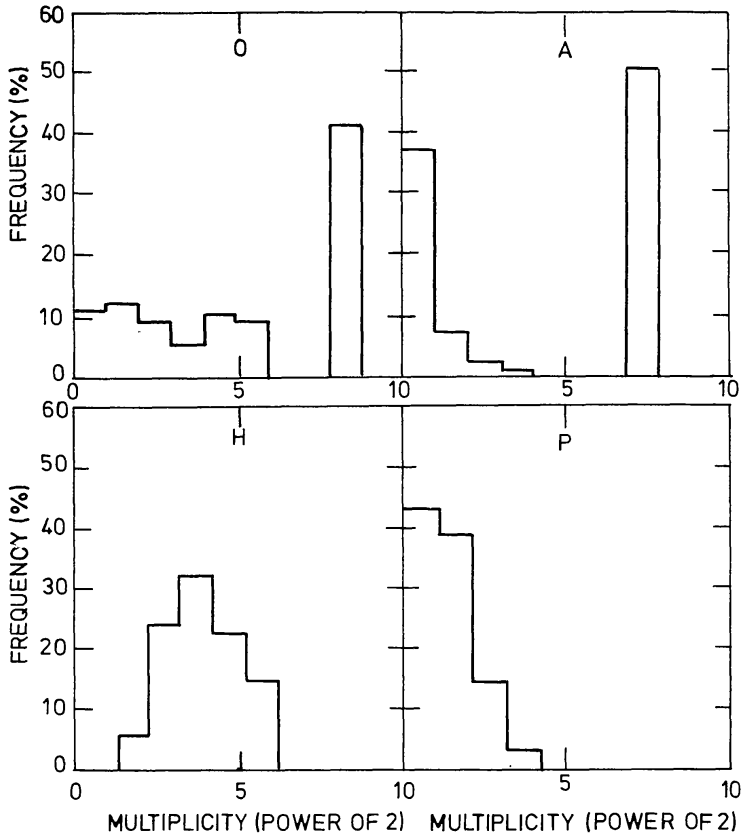

Figure 24 Distribution of multiplicity in "connected" systems (neighborhood radius 5 Mpc). The multiplicity is expressed in powers of 2 [courtesy of Zeldovich et al. (99)].

numbers in the connected systems as powers of 2. The most striking characteristics are the high peaks in O and A for one structure containing roughly half of all the systems. Nothing of this kind exists in H or P.

The authors conclude from their statistics that practically all galaxies lie in supercluster structures filling only a minor fraction ($\simeq 1\%$) of space. They conclude also that "in regions of lower than the average matter density no galaxy formation takes place at all." In these regions conditions favorable for formation of galaxies would not have occurred.

9.2 *Sizes, Shapes, and Velocity Dispersions*

Table 2 summarizes some data about the four superclusters—Local (or Virgo), Perseus, Coma, and Hercules—which have been studied most extensively; the relatively nearby Hydra-Centaurus supercluster discovered by Chincarini & Rood (14); some local "clouds" that do not contain clusters, and have much smaller masses, but may be considered as superclusters on the strength of their diameters and structures; and, finally, the largest known structure, the Corona Borealis supercluster. All numbers given should be considered with much reserve. In many cases they are no

© Annual Reviews Inc. • Provided by the NASA Astrophysics Data System

1983ARA&A..21..3730

Table 2 General data of some superclusters

Supercluster	r (Mpc)	Major diameter (Mpc)	$a:b$	σ (km s^{-1})
"Local" (disk)[a]	20	~40	6:1	~350
South galactic chain (B)	28	40	6:1	300
Cloud A	50	34	4:1	~800
Cloud C	70	38	1.5:1	—
Hydra-Centaurus	58	90	4:1	440
Perseus	100	75	ridges	~400
Coma	136	91 160	4:1 7:1	300
Hercules	200	140	?	—
Corona Borealis[b]	480	350	?	—

[a] From Tully (92). The major diameter quoted is derived from the "dispersion" in his Table 2, reduced to $H = 50$ and multiplied by 1.5 to make it roughly equivalent with the diameters quoted for the other superclusters.
[b] Bahcall & Soneira (9) No. 12.

more than rough estimates. The data for the Hydra-Centaurus supercluster rest on radial velocities of 9 Sc galaxies measured by Rubin et al. (69), and 8 groups and clusters observed by Sandage (70). It also contains the cluster Abell 1060.

Supplementing Table 2 there are now the data contained in the Center for Astrophysics (CfA) Survey (16), which give a much better insight in the statistical properties. At the time of writing, these data have not yet been properly analyzed, but a "first look" shows that the well-defined structures have major diameters ranging from about 10 to 90 (or possibly 160) Mpc. These values are quite in line with the data in Table 2, except that features smaller than 30 Mpc are not represented in that table. It should be noted that the smaller structures are usually not well defined, and may often be subunits in larger agglomerations. While most of the features are smaller than 40 Mpc for the velocity range 3000–6000 km s^{-1}, those in the 6000–10,000 km s^{-1} picture are all between 40 and 90 Mpc.

Most of the superclusters of Table 2 appear considerably elongated, with axial ratios of ~0.2. In the CfA survey, axial ratios range from about 0.2 to 0.9.

Even in the cases that look strongly flattened, we do not know whether the structure is prolate or a disk strongly inclined to the plane of the sky. In several cases, as for instance the Coma supercluster, the velocity dispersion is much smaller than should be observed if we were looking edgeways at a disk expanding at a rate comparable to the universal expansion. This may

© Annual Reviews Inc. • Provided by the NASA Astrophysics Data System

1983ARA&A..21..3730

indicate that we are dealing with a strongly prolate feature rather than a disk.

There is, however, another argument which speaks against the edge-on disk. In such a disk the average distance, and therefore also the average velocity, should be constant along the apparent filament. In both the Hercules and Coma superclusters there is on the contrary a pronounced variation from one end to the other. In Coma the velocity is roughly 6500 km s^{-1} at the low right-ascension end as against 7500 km s^{-1}, or perhaps even 8500 km s^{-1}, at the high right-ascension end (cf. Figures 10*b* and *c*). In Hercules it varies from 9000 to 11,000 km s^{-1} between the two groups of Abell clusters separated by 25°. It seems, therefore, that at least in these two cases the superclusters have prolate rather than disk shapes. Unfortunately, direct tests, such as could probably be made by photometric measurements, are still lacking. In some cases, such as in the principal branch of the Perseus supercluster, filamentary structures are clearly indicated (see Figures 14 and 16).

Photometric observations of strongly elongated superclusters aimed at finding their spatial structure, inclination to the line of sight, and internal motions would be most rewarding.

As indicated in Table 2, the velocity dispersions in the line of sight are generally small. It should be stressed that, although their smallness mitigates against disk models, these dispersions cannot be used to estimate depth along the line of sight, because Hubble expansion is unlikely to occur in the direction of minor axes.

Another important characteristic of superclusters is that they rarely show a clear concentration to a center. The Local supercluster, with the Virgo cluster near its center, may be the only known exception.

9.3 *Mixing Times*

On the supposition that the random velocities are similar in all directions, we can estimate the time it would at present take for an average galaxy or cluster to move from one end of a supercluster to the other. For the larger superclusters in Table 2 these times range from 100 to 500 × 10^9 years[3]—quite long compared to the age of the Universe, which is 17.6 × 10^9 years for a Universe with one tenth of the critical density. Internal systematic motions must of course have been much higher, because the features must have expanded to their present sizes. But it appears improbable that in a supercluster as a whole important mixing has taken place.

[3] Strictly, these times should be computed in expanding coordinates, and would depend on the general density of the Universe and the density excess of the supercluster, but the times mentioned should give a general indication of the mixing times concerned.

© Annual Reviews Inc. • Provided by the NASA Astrophysics Data System

1983ARA&A..21..3730

9.4 *Galaxy Types and Superclustering*

Giovanelli et al. (39) have found that the structure of the Perseus supercluster is better defined by early-type galaxies than by late-types, which show a much wider distribution (cf. Section 5 and Figure 16). It is unknown to the author whether other similar cases have been observed. The phenomenon is of importance for the understanding of the way in which superclusters have been formed (cf. Section 10).

An interesting experiment, which has received little notice, has been done by Cracovian scientists. It uses a method called "statistical reduction," and has been applied by S. Zięba (100) to investigate the clustering characteristics of galaxies of different types. He deduced that E and S0 galaxies have a much stronger clustering tendency than spirals, both on small scales of 0°.5 to 1° as well as on scales of 5° to 10°. While for spirals Zięba's "concentration index" does not differ appreciably from that of a random distribution on scales of 5° and larger, it is clearly different for the elliptical galaxies, showing that for these a clustering tendency persists up to at least 24°, which is the radius of the field investigated.

It should be noted that the region studied was the north galactic polar cap down to $b = 66°$, and that the results must therefore to a certain degree reflect the well-known phenomenon of the concentration of E and S0 galaxies in the central part of the Virgo cluster. It would be interesting to make the same analysis for some other regions.

9.5 *Orientation of Clusters and Galaxies*

Galaxy clusters are often strongly elongated. Carter & Metcalfe (13) and more recently Binggeli (11) have indicated that almost all clusters are measurably flattened, and that, on the average, their ellipticities are larger than those of elliptical galaxies. From Binggeli's data, the median projected ellipticity $(1-b/a)$ for his sample of 44 clusters is seen to be 0.42. He estimates that the median spatial ellipticity would be 0.61 if they are oblate spheroids, or 0.5 if they are prolate. Apparently, the flattening is not due to rotation [Dressler (27)], and they are, therefore, probably prolate. As a rule, the first-ranked (cD) galaxies are likewise elongated, and have orientations very similar to that of the surrounding cluster. This alignment, first found by Sastry (76), has been confirmed in many later cluster studies [e.g. Dressler (26)]. In their detailed investigation of 14 clusters, Carter & Metcalfe (13) showed that in 10 of the clusters the position angles of the central galaxies and clusters differed by less than 15°; only in one case was the deviation larger than 30°. We thus have two independent ways of determining the orientation of a cluster.

Clear evidence for a close correspondence between the position angles of

© Annual Reviews Inc. • Provided by the NASA Astrophysics Data System

1983ARA&A..21..3730

cluster major axes and the orientation of the supercluster chains in which they are situated has been noted in the Coma (Section 4.2) and Perseus superclusters (Section 5).

Binggeli (11) has made the important discovery that there is a striking general correlation between the orientation of a cluster's major axis and the direction to the nearest neighboring cluster if this neighbor is less than 30–40 Mpc away. The evidence is shown in Figure 25. That the correlation is

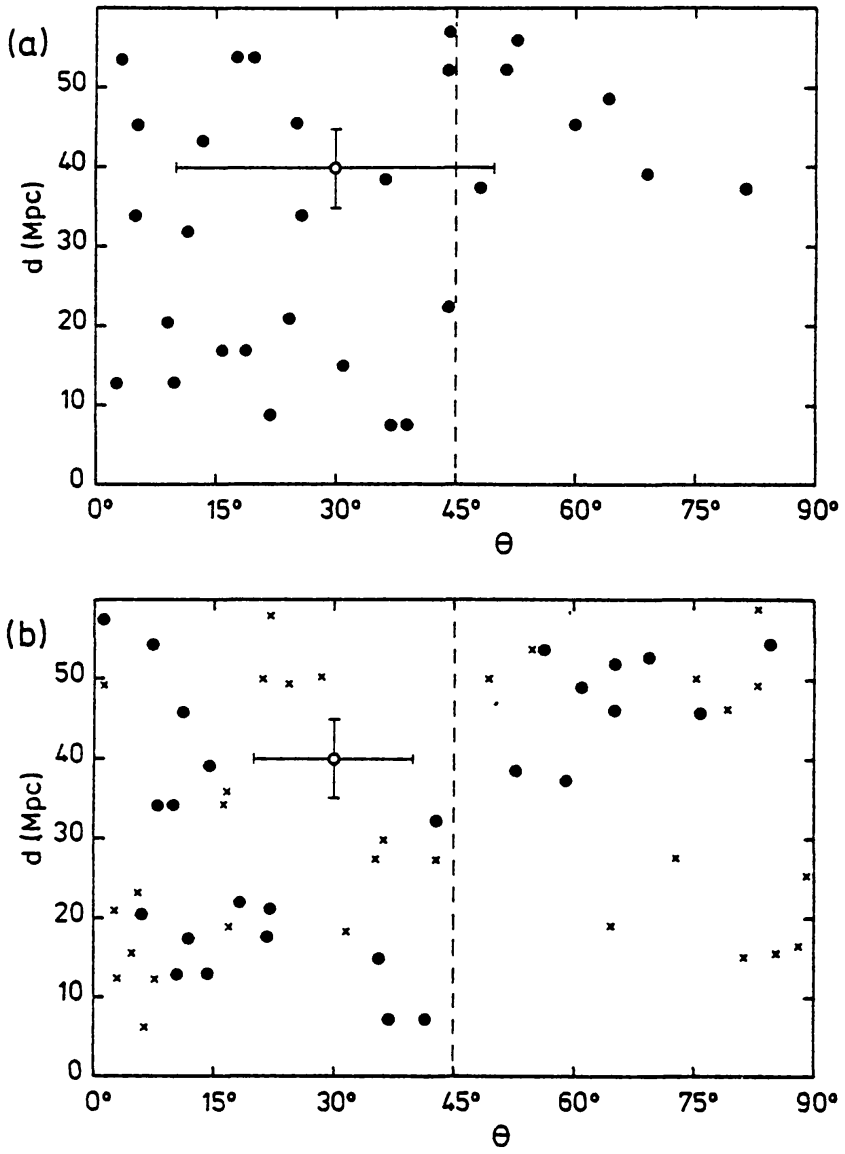

Figure 25 Relation between cluster position angles and direction to the nearest neighbor cluster. (*a*) Difference in position angle θ of the cluster major axis and the direction to the closest neighboring cluster as a function of the distance d to this neighbor; (*b*) same as for (*a*), except that the cluster position angle is replaced by the position angle of the major axis of the first-ranked galaxy. Crosses refer to clusters for which only the position angle of the first-ranked galaxy is known [from Binggeli (11)].

© Annual Reviews Inc. • Provided by the NASA Astrophysics Data System

1983ARA&A..21..3730

not caused by a partial overlap between neighboring clusters is shown by the lower diagram, where position angles of the first-ranked galaxies are used instead of cluster major axes. The effect is clearly present, but there are six discordant cases; however, four of these are clusters that have no observable elongation, and are therefore of no significance in the present context.

The fact that clusters tend to point to their nearest neighbor if they are closer than ~ 35 Mpc has important implications. The neighbors are apparently related. The relation might be their membership in the same supercluster. As is discussed in the next section, there are reasons to believe that superclusters originated by compression in the gaseous stage of the Universe, either as "pancakes" in the way advocated by the school of Zeldovich (97–99), or perhaps by a mechanism like that proposed by Ostriker & Cowie (62). In both cases the compression may well have been responsible for the flattened or elongated shapes of the superclusters, as well as for the elongation of the clusters formed in them.

Binggeli has also compared the orientation of a cluster with the directions toward more distant clusters in the surrounding volume of radius 100 Mpc, and has found that even up to 100 Mpc there is a distinct correlation, though much weaker than that observed for the nearest neighbors. This indicates that "relations" exist up to distances of 100 Mpc, distances of the same order as the major diameter of superclusters.

The evidence for a correlation of cluster properties over distances on the scale of superclusters is a strong argument for the view that superclusters formed prior to or simultaneously with the clusters contained within them.

The various attempts that have been made to find preferential orientations of *galaxies* within a supercluster have not yielded convincing results. In a recent analysis of the Local supercluster, MacGillavry et al. (53) found a "marginally significant" tendency for galaxies to be aligned along the plane of this supercluster. Gregory et al. (41), who have investigated the orientations in the Perseus supercluster, found that the distribution of position angles has two peaks, one roughly corresponding with the direction of the main filament, the other perpendicular to it.

A different phenomenon has been studied by Tifft (91). In a program of radial-velocity determinations of about 300 double galaxies, he investigated the distribution of the position angles of these doubles in relation to superstructures in which he judged them to be situated. He found indications that the position angles for doubles in the same region tend to be parallel, and possibly also parallel with the elongated superstructures; however, the evidence is not convincing, especially for the latter suggestion.

© Annual Reviews Inc. • Provided by the NASA Astrophysics Data System

1983ARA&A..21..3730

9.6 *Is There Intergalactic Gas in Superclusters?*

It is conceivable that some of the gas that contracted into superclusters (cf. Section 10) did not condense into galaxies, and remained as a thin intergalactic medium. Oort (60) advanced the hypothesis that the Lyman α absorption lines seen in distant quasars, which indicate H I column densities of the order of 10^{14} cm^{-2} (74), might be due to such gas. The idea was suggested by the circumstance that the average separation between the Lα absorptions was of the same order as that between superclusters on a line of sight. The close similarity between the two is confirmed by the much better supercluster statistics provided by the CfA survey (Section 4.3). However, the hypothesis appears to be contradicted by the recent observations of a pair of quasars separated by 187″, which at the distance of these quasars (at $z = 2.518$ and $z = 2.605$, respectively) corresponds to a separation between 1 and 2 Mpc, depending on the cosmological model. If the absorption lines originated in superclusters, the lines of sight to the two quasars should pass through the same superclusters, and the Lα redshifts should be practically identical in the two quasars. Actually, no correlation was observed [Sargent et al. (75)]. The Space Telescope will be needed to discover whether there is Lα absorption in known superclusters.

9.7 *Voids*

The study of superclusters is inextricably interwoven with the study of voids. In all regions where deep radial-velocity surveys have been made, the velocity distribution shows striking empty domains where over considerable ranges virtually no galaxies are found [cf. Figures 12 (Coma), 15 (Perseus), 18 and 19 (Hercules), and also Figure 10, where many similar empty spaces can be seen]. The diameters of the voids range up to ~ 100 Mpc.

A large void in Bootes was indicated by observations of faint galaxies by Kirshner et al. (50); supplementary observations by the same authors confirmed this approximately. The appearance of this underdense region is accentuated by two large superclusters: the Hercules supercluster on the near side, at z between 0.0031 and 0.0040; and the powerful Corona Borealis supercluster, containing 15 rich Abell clusters, at $z = 0.0065$ on the far side [Bahcall & Soneira (6)]. A void of a somewhat different nature, with much larger dimensions, has been indicated by Bahcall & Soneira (7) in the distribution of rich Abell clusters of distance groups 1–4. This apparent void, between $\ell \simeq 140°$ and 240°, $b \simeq 30°$ and 50° (cf. Figure 21), is $\sim 100°$ across the sky (corresponding to roughly 600 Mpc) and about 300 Mpc deep. It is not due to galactic absorption, but the possibility that it is a chance fluctuation cannot at present be excluded.

© Annual Reviews Inc. • Provided by the NASA Astrophysics Data System

1983ARA&A..21..3730

The voids are, in general, partly enveloped by concentrations of galaxies, identified with superclusters. Whether essentially all galaxies and clusters are confined to such superstructures, as several authors believe, or whether a sensible fraction is dispersed over the whole of space cannot yet be definitely answered.

The existence of large holes appears to be an important characteristic of the Universe. It is unknown whether the voids are actually empty, or whether they are regions where conditions have been unfavorable for galaxy formation, but which are nevertheless filled with invisible matter. We return to this problem in Section 10.

9.8 *Connections between Superclusters*

A question of prime importance for our insight into the Universe is whether superclusters are discrete entities, or whether they are interconnected and form some kind of semicontinuous pattern extending throughout space. From their study of the spatial distribution of galaxies and clusters in the southern galactic hemisphere, Einasto and coworkers (29) came to the conclusion that neighboring superclusters are in contact and contain common elements. The evidence that the various branches (or "filaments") of the complex structure in Perseus and surroundings are connected, and that they form part of one large "Perseus supercluster," seems convincing, but much further work on radial velocities would be needed to prove that they are also connected with surrounding superstructures. Thin strings of galaxies connecting the Virgo supercluster with the Coma supercluster have been displayed in (99) (cf. Section 3, Figure 7). An interesting case of a possible connection between two very large superclusters is that of Coma and Hercules, mentioned in Section 4.2. From an inspection of Figure 10, one gets the impression that many structures are fairly isolated.

The time does not yet seem ripe for an answer to the fundamental question of an overall interconnection between superclusters.

9.9 *Ages*

There is an indication that superclusters may have existed as early as $z \sim 3.0$ (cf. Section 8).

10. ORIGIN

10.1 *Introduction; Adiabatic vs Isothermal Fluctuations*

The central problem is the nature of the primeval density perturbations that formed the galaxies, clusters, and superclusters. Were they fluctuations in space curvature, in which radiation and matter were perturbed together (called "adiabatic"), or was only the matter density perturbed, the radiation

© Annual Reviews Inc. • Provided by the NASA Astrophysics Data System

1983ARA&A..21..3730

remaining nearly homogeneous (therefore "isothermal")? The adiabatic model is favored by theoreticians, but in the present state of knowledge isothermal perturbations cannot be excluded. The idea is that if the observed matter-antimatter asymmetry is created in the very early Universe by interactions from Grand Unification Theories, density perturbations after that epoch will be of the adiabatic type. Also, later generation of isothermal fluctuations from adiabatic ones seems to be quite inefficient.

In the case of adiabatic fluctuations, only those encompassing masses larger than $\simeq 10^{13}\ M_\odot$ survived. Smaller-mass perturbations are washed out by photon viscosity in the era before decoupling. Characteristic masses to be expected are $\simeq 10^{13}$–$10^{15}\ M_\odot$. It is suggestive that these are of the same order as the masses of superclusters. After the decoupling of matter and radiation, at $z \simeq 1000$, regions in which the density exceeds the "critical" or "closure" density of the Universe will expand to a maximum radius, and then collapse. Gas pressure is negligible up to the collapse stage; during the collapse the gas cools by radiation, and conditions may become favorable for the formation of galaxies and clusters. A supercluster may evolve.

It was early recognized that because the regions of excess density are unlikely to be precisely spherical, they would always collapse first along their smallest diameters and form what Zeldovich (97) termed "pancakes." If they further contract along their intermediate diameters, they would evolve into prolate structures.

According to Zeldovich, the birth of pancakes would occur from some high z (of the order of 10 or 20) up to $z \simeq 4$ or 3, and might well account for the high birthrate of quasars in the past. After the initial collapse, gas will still continue to stream into the pancakes, though at a reduced rate. The "cigars" and "pancakes" will, at least in their outer parts, continue to spread lengthwise and in their planes, and they may intersect. The Moscow astronomers have done much work, analytical as well as numerical, on predicting their subsequent evolution [cf. (98) and Doroshkevich et al. (23, 24)].

Several other authors have discussed the evolution of aspherical fluctuations in an expanding universe [cf. Icke (48), also quoted by Oort (59), White & Silk (94), Barrow & Silk (10), Palmer (63), and references in these articles].

Voids would form in an analogous manner from regions that were underdense, or had a higher than average expansion. An extensive discussion on the formation of holes has been given by Hoffman et al. (45), who showed that deep holes can form only if Ω is near unity, and that isolated spherical voids will be surrounded by dense, thin ridges. The authors comment on the problem of the large contrasts at recombination

© Annual Reviews Inc. • Provided by the NASA Astrophysics Data System

1983ARA&A..21..3730

required to form the observed holes and clusters, and the apparent conflict with the absence of such contrasts in the cosmic microwave background, a problem which is discussed in Section 10.2.

In the *isothermal hypothesis*, perturbations of all sizes can exist. It has generally been assumed that the largest density amplitudes will be found in perturbations of smallest mass, and that these will therefore be the first to collapse. At decoupling, the smallest masses into which the medium can fragment (the Jeans mass) are $\sim 10^6\ M_\odot$, of the order of globular-cluster masses. Some astronomers have speculated that these perturbations would develop into globular clusters, others that they would condense into supermassive "stars" (25, 65). The mutual attraction of these objects will have caused them to cluster, possibly into galaxies, which would in their turn have a tendency to cluster and form galaxy clusters or larger structures. But it is improbable that superclusters with dimensions of 100 Mpc could form in the time available unless, superposed on the small-scale isothermal fluctuations, perturbations on the scale of superclusters had been present initially. We would thus be led to a mixed scenario with additional large-scale density perturbations (from adiabatic fluctuations?).

The difference between the two theories can also be characterized by the following question: Were supercluster structures the first to form and did the galaxies form within these structures, or instead were the galaxies the first to come into existence, and did they gather into superclusters subsequently?

Observational astronomers have mostly favored the former picture, on the ground that the flat or filamentary structure of superclusters appeared to require dissipation of energy, which could only have occurred in the gaseous state. This argument has, however, lost its significance since it was shown that such structures can also form if there is no dissipation [cf. Dekel (17)].

But there is another fact of observation that gives a strong indication that galaxies and clusters pertaining to superclusters have formed only after the collapse of the supercluster mass while it was still in a gaseous state. This is the segregation of different galaxy types in the principal branch of the Perseus supercluster (cf. Section 5 and Figure 16, and Section 9.4). A similar segregation is found in large clusters. While in the inner parts of rich clusters the preponderance of E and S0 galaxies might be due to encounters, this cannot readily explain the phenomenon in the outer parts of the Virgo cluster, and certainly not the segregation in the Perseus supercluster.

A second indication of a similar nature is the apparent alignment of the major axes of galaxy clusters, discussed in Section 9.5.

In my opinion these facts argue in favor of the scenario in which superclusters formed first, and galaxies afterwards.

© Annual Reviews Inc. • Provided by the NASA Astrophysics Data System

1983ARA&A..21..3730

10.2 *Adiabatic Fluctuations*

There is, however, a serious difficulty with the adiabatic model: In order to get a timely collapse of the perturbed regions, an overdensity at the time of decoupling is required that is much larger than that corresponding to the observed upper limit of the fluctuations in the microwave background radiation.

In an Einstein-de Sitter Universe, the time of collapse of a spherical region of fractional overdensity $\eta (= \delta\rho/\rho)$ at decoupling (assumed to be at $z = 1000$) is

$$t_{\text{collapse}} = 1.90 \times 10^{-3}\, \eta^{-3/2},$$

if times are in units of 10^9 yr. The expression can be derived directly from Kepler's third law by using the definition of critical density [cf. (59), p. 398].

In an Einstein-de Sitter Universe, the collapse occurs at the present time ($t = 13.04$ in units of 10^9 yr) if $\eta = 0.0028$. If it is to collapse at $z = 5$ ($t = 0.89$), η must be taken to be 0.0166. These numbers apply to a Universe of critical density, where the main mass must consist of nonbaryonic matter (such as heavy neutrinos). If the Universe contains baryons only, the observed abundances of the light elements, made during the primordial nucleosynthesis, imply a density less than $0.1\ \rho_{\text{crit}}$; in that case, still larger fluctuations are required.

As pointed out in the preceding section, actual perturbations are likely to collapse into "pancake" or "cigar" shapes. The densest, inner regions which collapse first, will cool fastest, become ultimately Jeans unstable, and may fragment into galaxies. It is conceivable that due to the relatively quiescent conditions in these inner layers the galaxies formed would have little rotation, so that there would ensue a preponderance of ellipticals. The shock waves caused by the gas falling into the pancakes at later stages would tend to set up turbulence, so that galaxies formed in the outer regions would receive much angular momentum and become spirals [cf. (99)]. This might explain the segregation between early- and late-type galaxies, such as observed in the main branch of the Perseus supercluster.

However, it is doubtful whether this scenario can be viable in such a simple form. Detailed measurements of the microwave background radiation have shown it to be remarkably smooth. Except for the variation due to the Sun's motion, no fluctuations have been observed on any scale, including the scale of $\sim 10'$ that would be spanned by a supercluster of mass $10^{16}\ M_\odot$. The present upper limit for variations in $\delta T/T$ is 10^{-4}; some measurements have indicated even smaller upper limits. The corresponding upper limit for $\delta\rho/\rho$ is $\sim 3 \times 10^{-4}$, some 50 times smaller than what would be required for a collapse around $z = 5$ in an Einstein-de Sitter Universe. The real discrepancy may be somewhat less, because not all "waves" at

© Annual Reviews Inc. • Provided by the NASA Astrophysics Data System

1983ARA&A..21..3730

decoupling need be equally high: some may collapse only at the present epoch, or even later. There are other possibilities to reduce the discrepancy, but at best by only a factor of ~ 3, while on the other hand the real fluctuation in $\delta T/T$ may well be smaller than the quoted upper limit. It should be pointed out that it is not only the origin of superclusters that is faced with this difficulty, but also that of single clusters.

There are two ways out of the dilemma. One is that the mass of the Universe consists mostly of weakly interacting particles (such as neutrinos with a mass of the order of 10 eV, for example). In this case, perturbations can start to evolve when these particles become nonrelativistic, which may be much earlier than the epoch at which the baryons decouple from radiation. Adiabatic perturbations can then collapse at sufficiently early epochs without entailing large fluctuations in the baryon density at decoupling. The fluctuations $\delta T/T$ could in this scenario remain well below the upper limit indicated by the observations. The collapse differs from that of a baryon gas in that there is no dissipation. As has been mentioned in the preceding section, very dense structures can nevertheless be formed from the smooth initial perturbations. The freely falling particles will concentrate into "caustics," surrounded by extended halos. Just as in the baryon-dominated case, pancakes, filaments, and knots will be formed. Numerical experiments, quoted in (99), confirm that the knots attain the highest density, the filaments the next highest, and the pancakes the least.

Baryons would flow into the potential wells formed by the "neutrinos," and galaxies may be formed in the same way as sketched in the foregoing. We would therefore have neutrino pancakes and cigars, with baryon pancakes and filaments inside [cf. Doroshkevich et al. (22)]. For discussions of the role of neutrinos, see also Szalay (87) and Novikov (58).

The second way in which the problem of the discrepancy between the existence of clusters and superclusters and the lack of corresponding fluctuations in the 3-K background might be solved is by assuming that the intergalactic medium was reheated after the decoupling. The dense ionized gas might then scatter the background radiation, so that the fluctuations would be smeared out. In order to be effective, such reionization should have taken place at an early epoch ($z \gtrsim 10$) when the density was still sufficiently high [cf. (45)].

A severe problem is the question of where the ionizing radiation could have come from. Quasars were born much too late. A new type of ultraviolet source, formed in an early phase, would therefore have to be devised. It has been speculated that superposed on the large-scale adiabatic perturbations there would have been isothermal fluctuations, which would have had smaller masses and larger amplitudes. The earliest things to form would then probably have masses of the order of the Jeans mass at

© Annual Reviews Inc. • Provided by the NASA Astrophysics Data System

1983ARA&A..21..3730

decoupling ($\sim 10^6$–10^8 $M_\odot$). It is conceivable that these would condense into starlike objects. Such objects, called Population III, have been widely discussed in connection with the formation of halos of galaxies. It may be hypothesized that such early superstars would have produced enough far-ultraviolet radiation to reionize the intergalactic medium at $z > 10$. Rees (66) has made the interesting suggestion that if the medium in the large voids were ionized in this manner it could have effectively prevented the formation of galaxies, which might explain the almost complete lack of luminous matter in the voids.

In the present state of our knowledge, the various ad-hoc hypotheses involved would seem to make the "scattering" hypothesis less attractive than that of the heavy neutrinos.

10.3 *Multiparticle Simulations*

Much of the clustering in the Universe has probably been caused by the gravitational interaction between protogalaxies. Impressive demonstrations of how this interaction can make clumpiness on all scales up to about 10 Mpc have been produced by many-body simulations. An example, from an investigation by Aarseth et al. (1), is shown in Figure 26. Their calculations were started with an essentially Poisson distribution at an epoch when the scale of the Universe was 1/31.9th of the present scale, and its age was 0.2×10^9 yr (for $H_0 = 50$ km s^{-1} Mpc^{-1}, $\Omega = 0.1$). The left-hand side of the figure is for a time when the scale had increased to twice that at the start; the right-hand side is for the present epoch. The authors have shown that by a judicious, and plausible (considering the estimated collapse time for known galaxies), choice of the starting epoch the observed covariance function of the galaxy distribution can be well reproduced. Most of the clumps and clusters form already in the first tenth of the time span covered. Beside agglomerations, large voids are also produced.

Simulations for a universe with $\Omega = 1$ gave very similar results.

Extensive experiments along the same general lines have since been made and discussed by Efstathiou & Eastwood (28). Some of their models contained 20,000 particles. They found similar structures, but too high relative velocities of the correlated galaxies. Recently, Miller (54) has shown results of integrations for 100,000 particles, which impressively demonstrate the small-scale clustering, the formation of large spherelike voids, as well as of elongated features, and the second-order clustering, which appears to extend over a large part of the region investigated.

All these results show so much resemblance to the observed distribution that at first sight it is tempting to conclude that perhaps all structure in the Universe could have been produced by the mutual gravitation of galaxies that were initially distributed at random, so that there might be no need for

© Annual Reviews Inc. • Provided by the NASA Astrophysics Data System

1983ARA&A..21..3730

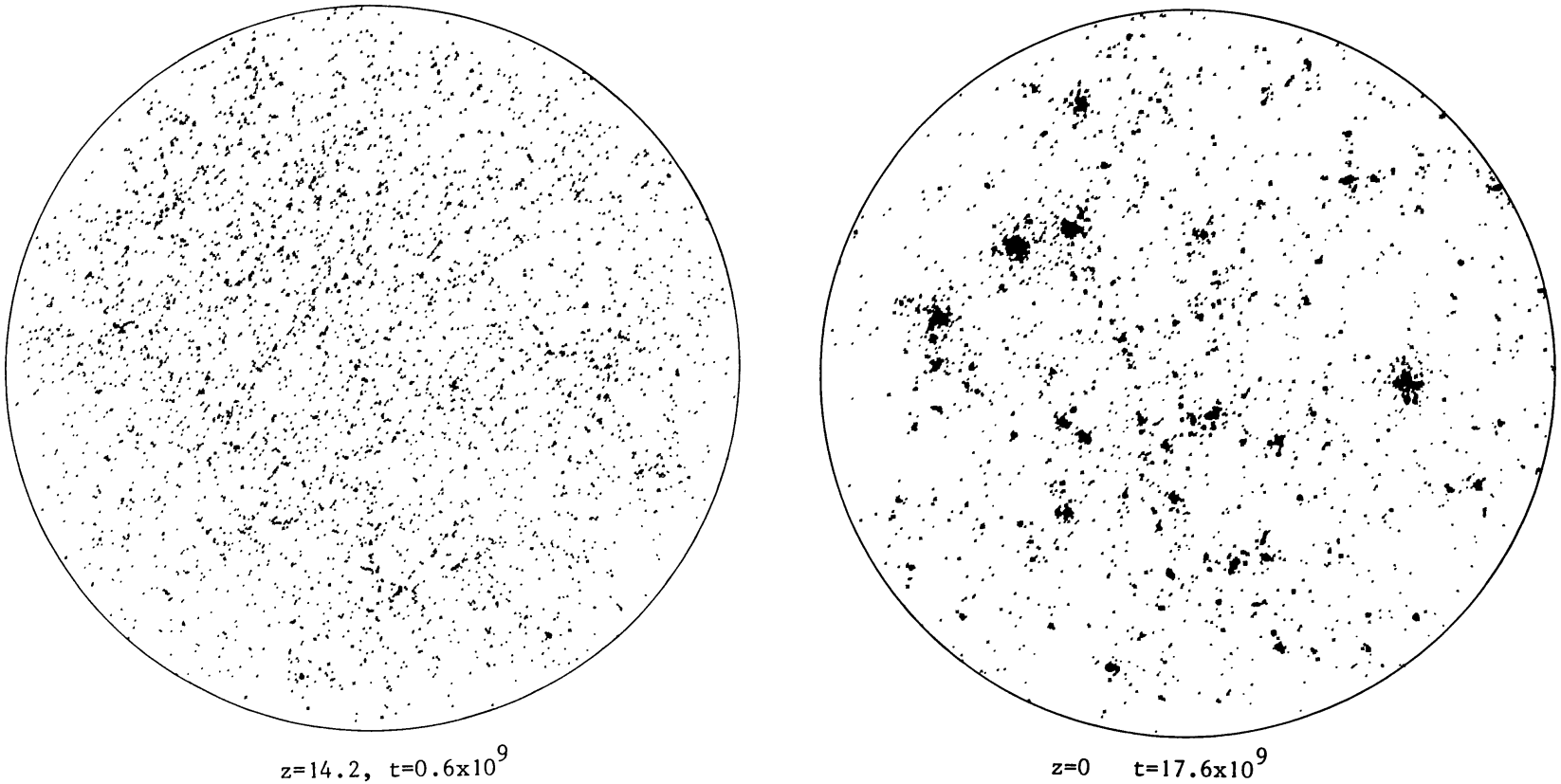

Figure 26 N-body simulation of galaxy clustering. A sphere of present radius 50 Mpc containing 4000 galaxies in comoving coordinates. The x- and y-coordinates of the galaxies are plotted with the z-coordinate suppressed. $\Omega = 0.1$, $H_0 = 50$ km s^{-1} Mpc^{-1}. (*Left*) $z = 14.2$, (*right*) $z = 0$. Courtesy of Aarseth et al. (1) and the *Astrophysical Journal*.

© Annual Reviews Inc. • Provided by the NASA Astrophysics Data System

1983ARA&A..21..3730

large-scale adiabatic perturbations. This, however, does not seem possible. Given the earliest epoch at which protogalaxies could plausibly have become separate entities, and the consequent limited range of the possible expansion factor, no structures of supercluster size ($\simeq 100$ Mpc) can have formed in this manner. Moreover, it is difficult to see how a segregation of different galaxy types and an alignment of cluster major axes could have been produced by the mutual attraction of galaxies.

The latter, however, must have strongly affected the distribution of galaxies and clusters *within* the superclusters, and have caused most of the observed clumpiness.

An interesting experiment was carried out by Frenk et al. (36). They made multiparticle simulations with large cutoff lengths for the initial perturbations, mimicking the adiabatic ("pancake") theory. By choosing an appropriate cutoff length, they obtained final distributions that closely resemble observed supercluster structures. For details, see the original article.

Another mechanism which may have been important for the galaxy distribution is that described by Ostriker & Cowie (62), who considered the effect that the birth of a major galaxy will have on a surrounding intergalactic medium. They noted that the energy released by the massive stars in such a galaxy, when propagating through the medium, will finally result in a slow-moving expanding shell having a mass of 10^2–10^3 times the mass of the parent galaxy. A second generation of galaxies may form in this shell. The authors showed that at appropriate eras in the evolution of the Universe this can lead to a chain reaction and extended structures might be built up. Whether these could grow to sizes of superclusters is, however, doubtful.

For the present author the main problems are the origin of the "seed" galaxies needed to start the compression processes, and why, if such seeds could be formed, were not all galaxies formed in the same way. Seed galaxies will in any case appear upon the collapse of pancakes. Processes such as those considered by Ostriker & Cowie may thus have started after the birth of the earliest pancakes, albeit under somewhat different conditions.

11. THE DENSITY OF THE UNIVERSE

Several attempts have been made to determine the mass density of the Universe from the motions and density distribution in superclusters (in particular the Local supercluster). As the results are uncertain and the subject lies at the boundary of this review, it seems premature to discuss them in the present volume.

© Annual Reviews Inc. • Provided by the NASA Astrophysics Data System

1983ARA&A..21..3730

12. CONCLUSIONS

Superclusters are unrelaxed structures. They have no symmetry and no central concentration. Their complicated nature is illustrated by the Local (Virgo), the Coma, Perseus, and Hercules superclusters. Their space frequency and general properties can be derived from the *Redshift Catalog of the Center for Astrophysics* (cf. Section 4). Many superclusters seem to be very elongated. Typical (baryon) masses for the larger structures are $\sim 10^{15}$–$10^{16}\ M_{\odot}$. The very large sizes—up to 350 Mpc—indicate that they descend from primeval density fluctuations.

There are indications that the great majority of galaxies are concentrated in superclusters, and that the spaces in between are virtually devoid of luminous matter.

Particularly interesting is the evidence for segregation of galaxy types in the Perseus supercluster, and the indication that the major axes of rich clusters tend to be oriented along the main features of superclusters. These facts suggest that superclusters formed by a collapse in the gaseous stage, prior to the birth of galaxies, and that they came from adiabatic perturbations in the early Universe. The fact that no corresponding fluctuations are seen in the microwave background radiation indicates either that the main mass of the Universe consists of weakly interacting particles, such as heavy neutrinos, or that the background fluctuations have been washed out by a reionization of intergalactic gas fairly soon after decoupling.

ACKNOWLEDGMENTS

In preparing this review, I have greatly profited from discussions with many colleagues; in particular, I wish to thank Neta Bahcall, A. Dekel, J. Einasto, R. Giovanelli, C. Norman, M. Rees, and H. Rood for their valuable suggestions. To F. Klinkhamer and T. de Zeeuw I am indebted for their careful reading of the manuscript and the improvements to which this has led. Many astronomers have sent me preprints, which have been invaluable for the preparation of the manuscript; I have especially profited from that of the article by Zeldovich et al. (99).

I am greatly indebted to J. Bahcall for his hospitality at the Institute for Advanced Study in Princeton, where most of the last part of this review was prepared.

Literature Cited

1. Aarseth, S. J., Gott, J. R. III, Turner, E. L. 1979. *Ap. J.* 228:664
2. Abell, G. O. 1958. *Ap. J. Suppl.* 3: 211
3. Abell, G. O. 1961. *Astron. J.* 66:607
4. Arp, H. C. 1980. In *Texas Symp. Relativ. Astrophysics, 9th, Ann. NY Acad. Sci.* 336:94
5. Bahcall, N. A. 1977. *Ann. Rev. Astron. Astrophys.* 15:505
6. Bahcall, N. A., Soneira, R. M. 1982. *Ap. J. Lett.* 258:L17

© Annual Reviews Inc. • Provided by the NASA Astrophysics Data System

1983ARA&A..21..3730

7. Bahcall, N. A., Soneira, R. M. 1982. *Ap. J.* 262:419
8. Bahcall, N. A., Soneira, R. M. 1983. *Ap. J.* 270: In press
9. Bahcall, N. A., Soneira, R. M. 1983. *Ap. J.* Submitted for publication
10. Barrow, J. D., Silk, J. 1981. *Ap. J.* 250:432
11. Binggeli, B. 1982. *Astron. Astrophys.* 107:338
11a. Burbidge, E. M., Junkkarinen, V. T., Koski, A. T., Smith, H. E., Hoag, A. A. 1980. *Ap. J. Lett.* 242:L55
12. Burns, J. O., Owen, F. N. 1979. *Astron. J.* 84:1478
13. Carter, D., Metcalfe, N. 1980. *MNRAS* 191:325
14. Chincarini, G., Rood, H. J. 1979. *Ap. J.* 230:648
15. Chincarini, G., Rood, H. J., Thompson, L. A. 1981. *Ap. J. Lett.* 249:L47
16. Davis, M., Huchra, J., Latham, D. W., Tonry, J. 1982. *Ap. J.* 253:423
17. Dekel, A. 1983. *Ap. J.* 264:373
18. Deleted in proof
19. de Vaucouleurs, G. H. 1956. *Vistas Astron.* 2:1584
20. de Vaucouleurs, G. H. 1975. In *Galaxies and the Universe* (*Stars and Stellar Systems*, Vol. 9), ed. A. Sandage, M. Sandage, J. Kristian, G. A. Tammann, pp. 557–600. Univ. Chicago Press
21. de Vaucouleurs, G. H. 1978. In *The Large-Scale Structure of the Universe, IAU Symp. No. 79*, ed. M. S. Longair, J. Einasto; pp. 205–13
22. Doroshkevich, A. G., Khlopov, M. Yu., Sunyaev, R. A., Szalay, A. S., Zeldovich, Ya. B. 1981. *Texas Symp. Relativ. Astrophys., 10th, Ann. NY Acad. Sci.* 375:32
23. Doroshkevich, A. G., Saar, E. M., Shandarin, S. F. 1978. In *The Large-Scale Structure of the Universe, IAU Symp. No. 79*, ed. M. S. Longair, J. Einasto, pp. 423–25
24. Doroshkevich, A. G., Shandarin, S. F., Saar, E. M. 1978. *MNRAS* 184:643
25. Doroshkevich, A. G., Zeldovich, Ya. B., Novikov, I. D. 1967. *Sov. Astron.* 11:233
26. Dressler, A. 1978. *Ap. J.* 226:55
27. Dressler, A. 1981. *Ap. J.* 243:26
28. Efstathiou, G., Eastwood, J. W. 1981. *MNRAS* 194:503
29. Einasto, J., Jôeveer, M., Saar, E. 1980. *MNRAS* 193:353
30. Einasto, J., Klypin, A., Shandarin, S. 1983. See Einasto, J. 1983. In *Early Evolution of the Universe and its Present Structure, IAU Symp. No. 104*, ed. G. Chincarini, G. Abell, p. 405
31. Fetisova, T. S. 1981. *Astron. Zh.* 58:1137
32. Fisher, J. R., Tully, R. B. 1981. *Ap. J. Suppl.* 47:139
33. Focardi, P., Marano, B., Vettolani, G. 1982. *Astron. Astrophys.* 113:15
34. Fontanelli, P. 1982. In *The Comparative HI Content of Normal Galaxies*, ed. M. Haynes, R. Giovanelli, pp. 112–15. Green Bank, W.Va: Natl. Radio Astron. Obs.
35. Ford, H. C., Harms, R. J., Ciardullo, R., Bartko, F. 1981. *Ap. J. Lett.* 245:L53
36. Frenk, C. S., White, S. D. M., Davis, M. 1983. Preprint. Cf. also White, S. D. M. 1983. In *Internal Kinematics and Dynamics of Galaxies, IAU Symp. No. 100*, ed. E. Athanassoula, pp. 385–86
37. Giovanelli, R. 1983. In *Early Evolution of the Universe and its Present Structure, IAU Symp. No. 104*, ed. G. Chincarini, G. Abell, p. 273
38. Giovanelli, R., Haynes, M. P. 1982. *Astron. J.* 87:1355
39. Giovanelli, R., Haynes, M. P., Chincarini, G. L. 1983. In preparation
40. Gregory, S. A., Thompson, L. A. 1978. *Ap. J.* 222:784
41. Gregory, S. A., Thompson, L. A., Tifft, W. G. 1981. *Ap. J.* 243:411
42. Groth, E. J., Peebles, P. J. E. 1977. *Ap. J.* 217:385
43. Hauser, M. G., Peebles, P. J. E. 1973. *Ap. J.* 185:757
44. Hoessel, J. G., Gunn, J. E., Thuan, T. X. 1980. *Ap. J.* 241:486
45. Hoffman, G. L., Salpeter, E. E., Wasserman, I. 1983. In *Early Evolution of the Universe and its Present Structure, IAU Symp. No. 104*, ed. G. Chincarini, G. Abell, p. 211
46. Hubble, E. P. 1934. *Ap. J.* 79:8
47. Huchra, J. P., Davis, M., Latham, D. W., Tonry, L. J. 1983. *Ap. J. Suppl.* 52(2): In press
48. Icke, V. 1973. *Astron. Astrophys.* 27:1
49. Jôeveer, M., Einasto, J., Tago, E. 1978. *MNRAS* 185:357
50. Kirshner, R. P., Oemler, A., Schechter, P. L., Shectman, S. A. 1981. *Ap. J. Lett.* 248:L57
51. Longair, M. S. 1978. In *The Large–Scale Structure of the Universe, IAU Symp. No. 79*, ed. M. S. Longair, J. Einasto, pp. 305–14
52. Lucey, J. R., Dickens, R. J., Dawe, J. A., Mitchell, R. J. 1983. *MNRAS*. In press
53. MacGillavry, H. T., Dodd, R. J., McNally, B. V., Corwin, H. G. Jr. 1982. *MNRAS* 198:605
54. Miller, R. H. 1983. *Ap. J.* Submitted for publication; Cf. also Miller, R. H. 1983. In *Early Evolution of the Universe and its Present Structure, IAU Symp. No. 104*, ed. G. Chincarini, G. Abell, p. 411
55. Murray, S. S., Forman, W., Jones, C.,

© Annual Reviews Inc. • Provided by the NASA Astrophysics Data System

1983ARA&A..21..3730

Giacconi, R. 1978. *Ap. J. Lett.* 219:L89
56. Neyman, J., Scott, E. L., Shane, C. D. 1953. *Ap. J.* 117:92
57. Nilson, P. 1973. *Uppsala General Catalogue of Galaxies, Uppsala Obs. Ann.* 6
58. Novikov, I. D. 1983. In *Early Evolution of The Universe and its Present Structure, IAU Symp. No. 104*, ed. G. Chincarini, G. Abell, p. 457
59. Oort, J. H. 1970. *Astron. Astrophys.* 7:381
60. Oort, J. H. 1981. *Astron. Astrophys.* 94:359
61. Oort, J. H., Arp, H. C., de Ruiter, H. 1981. *Astron. Astrophys.* 95:7
62. Ostriker, J. P., Cowie, L. L. 1981. *Ap. J. Lett.* 243:L127
63. Palmer, Ph. L. 1981. *MNRAS* 197:721
64. Peebles, P. J. E. 1980. *The Large-Scale Structure of the Universe*, Princeton, N.J: Princeton Univ. Press
65. Peebles, P. J. E., Dicke, R. H. 1968. *Ap. J.* 154:891
66. Rees, M. J. 1983. In *Early Evolution of the Universe and its Present Structure, IAU Symp. No. 104*, ed. G. Chincarini, G. Abell, p. 299
67. Rood, H. J. 1976. *Ap. J.* 207:16
68. Rood, H. J., Sastry, G. N. 1971. *Publ. Astron. Soc. Pac.* 83:313
69. Rubin, V. C., Ford, W. K., Thonnard, N., Roberts, M. S., Graham, J. A. 1976. *Astron. J.* 81:687
70. Sandage, A. 1975. *Ap. J.* 202:563
71. Sandage, A., Tammann, G. A. 1981. *A Revised Shapley-Ames Catalog of Bright Galaxies, Carnegie Inst. Washington Publ. 633*
72. Sandage, A., Tammann, G. A. 1982. In *Astrophysical Cosmology*, ed. H. A. Brück, G. V. Coyne, M. S. Longair. *Pontif. Acad. Sci. Scr. Varia* 48:23
73. Sarazin, C. L., Rood, H. J., Struble, M. F. 1982. *Astron. Astrophys. Lett.* 108:L7
74. Sargent, W. L. W., Young, P. J., Boksenberg, A., Tytler, D. 1980. *Ap. J. Suppl.* 42:41
75. Sargent, W. L. W., Young, P., Schneider, D. P. 1982. *Ap. J.* 256:374
76. Sastry, G. N. 1968. *Publ. Astron. Soc. Pac.* 80:252
77. Schipper, L., King, I. R. 1978. *Ap. J.* 220:798
77a. Schneider, D. P., Gunn, J. E., Hoessel, J. G. 1983. *Ap. J.* 264:337
78. Seldner, M., Peebles, P. J. E. 1978. *Ap. J.* 225:7
79. Shane, C. D. 1975. In *Galaxies and the Universe, Stars and Stellar Systems*, ed. A. Sandage, M. Sandage, J. Kristian, 9:647–63
80. Shane, C. D., Wirtanen, C. A. 1967. *Publ. Lick Obs.* 22, Part 1
81. Shapley, H. 1930. *Harvard Obs. Bull. No. 874*, p. 9
82. Shapley, H. 1934. *MNRAS* 94:791
83. Shapley, H. 1935. *Harvard Obs. Ann.* 88:107
84. Shapley, H., Ames, A. 1932. *Harvard Obs. Ann.* 88(4):43
85. Soneira, R. M., Peebles, P. J. E. 1978. *Astron. J.* 83:845
86. Struble, M. F., Rood, H. J. 1982. *Astron. J.* 87:7
87. Szalay, A. 1983. In *Early Evolution of the Universe and its Present Structure, IAU Symp. No. 104*, ed. G. Chincarini, G. Abell, p. 307
88. Tarenghi, M., Chincarini, G., Rood, H. J., Thompson, L. A. 1980. *Ap. J.* 235:724
89. Tarenghi, M., Tifft, W. G., Chincarini, G., Rood, H. J., Thompson, L. A. 1979. *Ap. J.* 234:793
90. Thompson, L. A., Gregory, S. A. 1983. In preparation
91. Tifft, W. G. 1980. *Ap. J.* 239:445
92. Tully, R. B. 1982. *Ap. J.* 257:389
93. Webster, A. 1977. In *Radio Astronomy and Cosmology, IAU Symp. No. 74*, ed. D. L. Jauncey, pp. 75–79
93a. Webster, A. 1982. *MNRAS* 199:683
94. White, S. D. M., Silk, J. 1979. *Ap. J.* 231:1
95. Wilkinson, D. T. 1983. In *Early Evolution of the Universe and its Present Structure, IAU Symp. No. 104*, ed. G. Chincarini, G. Abell, p. 143
96. Yahil, A., Sandage, A., Tammann, G. A. 1980. *Ap. J.* 242:448
97. Zeldovich, Ya. B. 1970. *Astron. Astrophys.* 5:84
98. Zeldovich, Ya. B. 1978. In *The Large-Scale Structure of the Universe, IAU Symp. No. 79*, ed. M. S. Longair, J. Einasto, pp. 409–21
99. Zeldovich, Ya. B., Einasto, J., Shandarin, S. F. 1982. *Nature* 300:407
100. Zięba, S. 1977. *Acta Cosmologica* 6:75; Cf also Rudnicki, K., Zięba, S. 1978. In *The Large-Scale Structure of the Universe, IAU Symp. No. 79*, ed. M. S. Longair, J. Einasto, pp. 229–39
101. Zwicky, F., Wild, P., Herzog, E., Karpowicz, M., Kowal, C. T. 1961–1968. *Catalogue of Galaxies and Clusters of Galaxies*, Vols. 1–6. Pasadena: Calif. Inst. Technol.

© Annual Reviews Inc. • Provided by the NASA Astrophysics Data System